

**BATCH STUDY AND EXPERIMENTAL DESIGN FOR THE  
REMOVAL OF REACTIVE ORANGE 16 FROM AQUEOUS  
SOLUTION USING CHITOSAN BEADS**

By

**TONG JIN YING**

A project report submitted to the Department of Chemical Science

Faculty of Science

Universiti Tunku Abdul Rahman

in partial fulfilment of the requirements for the degree of

Bachelor of Science (Hons) Chemistry

May 2024

## **ABSTRACT**

### **BATCH STUDY AND EXPERIMENTAL DESIGN FOR THE REMOVAL OF REACTIVE ORANGE 16 FROM AQUEOUS SOLUTION USING CHITOSAN BEADS**

**TONG JIN YING**

Dye contamination of wastewater poses serious risks to the environment and has detrimental effects on the human health as well. In this research, the feasibility of using chitosan beads as promising adsorbent for the removal of Reactive Orange 16 was studied. Several factors such as contact time, initial concentration of dye, adsorbent dosage, agitation rate and pH were included in batch adsorption studies to examine their impact towards the adsorption process. The characterization study on the synthesized chitosan beads was carried out using Attenuated Total Reflectance-Fourier Transform Infrared (ATR-FTIR) spectroscopy, Scanning Electron Microscopy (SEM) and Atomic Force Microscopy (AFM). The equilibrium adsorption data was found to be best fitted to both Langmuir and BET isotherm model with  $R^2$  value of 0.9940 and maximum adsorption capacity of 38.17 mg/g. Besides, the adsorption of RO16 by chitosan beads followed the pseudo-second order kinetic model. Modification on the chitosan beads was performed by adding polyethylene

glycol (PEG) to evaluate its adsorption performance. Plackett-Burman design was used to identify the significant factors in the adsorption process whereas RSM was utilized for the optimization study. The percentage uptake of RO16 can achieve up to 94.55% under optimum conditions of pH 3, 360 minutes of contact time, initial dye concentration of 100 mg/L, adsorbent dosage of 0.05 g and agitation rate of 150 rpm.

## **ABSTRAK**

### **KAJIAN KUMPULAN DAN REKA BENTUK EKSPERIMEN UNTUK PENYINGKIRAN REAKTIF OREN 16 DARIPADA LARUTAN AKUEUS MENGGUNAKAN MANIK KITOSAN**

**TONG JIN YING**

Pencemaran bahan pewarna dalam air kumbahan menimbulkan risiko yang serius kepada alam sekitar dan mempunyai kesan buruk kepada kesihatan manusia serta ekosistem. Dalam penyelidikan ini, kebolehlaksanaan menggunakan manik kitosan sebagai penjerap untuk penyingkiran Reaktif Oren 16 telah dikaji. Beberapa faktor telah dimasukkan dalam kajian penjerapan kelompok untuk mengkaji kesannya terhadap proses penjerapan, termasuk masa sentuhan, kepekatan awal pewarna, dos penjerap, kadar pengadukan dan pH. Manik kitosan yang disintesis telah dianalisis oleh spektroskopi Inframerah Transformasi Jumlah Reflektansi-Fourier (ATR-FTIR), Mikroskop Elektron Pengimbasan (SEM) dan Mikroskop Kekuatan Atom (AFM). Data penjerapan keseimbangan didapati paling sesuai untuk kedua-dua model isoterma Langmuir dan BET dengan nilai  $R^2$  0.9940 dan kapasiti penjerapan maksimum 38.17 mg/g. Selain itu, penjerapan RO16 oleh manik kitosan dipadankan dengan model kinetik pseudo-second order. Pengubahsuaian pada permukaan manik

kitosan dengan menambahkan polietilena glikol (PEG) juga dilakukan untuk menilai prestasi penjerapan. Reka bentuk Plackett-Burman digunakan untuk mengenal pasti faktor penting dalam proses penjerapan manakala RSM digunakan untuk pengoptimuman parameter proses. Peratusan pengambilan RO16 boleh mencapai sehingga 94.55% dalam keadaan optimum pH 3, 360 minit masa sentuhan, kepekatan pewarna awal 100 mg/L, dos penjerap 0.05 g dan kadar pengadukan 150 rpm.

## ACKNOWLEDGEMENT

In this acknowledgement for my thesis, I extend my appreciation to all those who have been part of this journey.

First of all, I would like to express my deepest appreciation to my supervisor, Dr Ong Siew Teng for her guidance and dedicated involvement in every step throughout the process. Words cannot express my gratitude to her, who generously provided knowledge, expertise and most importantly unwavering support throughout this journey. This endeavor would not have been possible without her.

I would also like to take this opportunity to thanks all the laboratory officers for providing assistance and feedback throughout this project. Their willingness and enthusiasm to assist in any way they could had encouraged me throughout the research project.

I would be remiss in not mentioning my friends and family, especially my parents for the unceasing encouragement, support and attention. Their belief in me has kept my spirits and motivation high during this process. I am grateful for all the ongoing support, emotional encouragement as well as the helpful advice that have provided to me throughout this time.

Last but not least, I would like to acknowledge the research facilities provided by UTAR. From the bottom of my heart, I sincerely thank everyone.

Thank you.

## DECLARATION

I hereby declare that this final year project report is based on my original work except for quotations and citations which have been duly acknowledged. I also declare that it has not been previously or concurrently submitted for any other degree at UTAR or other institutions.



*Jos.*

---

## APPROVAL SHEET

This final year project report entitled “**BATCH STUDY AND EXPERIMENTAL DESIGN FOR THE REMOVAL OF REACTIVE ORANGE 16 FROM AQUEOUS SOLUTION USING CHITOSAN BEADS**” was prepared by TONG JIN YING and submitted as partial fulfilment of the requirements for the degree of Bachelor of Science (Hons) Chemistry at Universiti Tunku Abdul Rahman.

Approved by:

*Ong S7*

---

(Dr. ONG SIEW TENG)

Date: 15/05/2024

Supervisor

Department of Chemical Science

Faculty of Science

Universiti Tunku Abdul Rahman



**FACULTY OF SCIENCE**

**UNIVERSITI TUNKU ABDUL RAHMAN**

Date: 13 May 2024

**PERMISSION SHEET**

It is hereby certified that **TONG JIN YING** (ID No: 20ADB02061) has completed this final year project report thesis entitled “BATCH STUDY AND EXPERIMENTAL DESIGN FOR THE REMOVAL OF REACTIVE ORANGE 16 FROM AQUEOUS SOLUTION USING CHITOSAN BEADS” under the supervision of Dr. ONG SIEW TENG from the Department of Chemical Science, Faculty of Science.

I hereby give permission to the University to upload the softcopy of my final year project report thesis in pdf format into the UTAR Institutional Repository, which may be made accessible to the UTAR community and public.

Yours truly,



---

(TONG JIN YING)

## TABLE OF CONTENTS

	<b>Page</b>
<b>ABSTRACT</b>	<b>ii</b>
<b>ACKNOWLEDGEMENT</b>	<b>vi</b>
<b>DECLARATION</b>	<b>vii</b>
<b>APPROVAL SHEET</b>	<b>viii</b>
<b>PERMISSION SHEET</b>	<b>ix</b>
<b>TABLE OF CONTENTS</b>	<b>x</b>
<b>LIST OF TABLES</b>	<b>xiii</b>
<b>LIST OF FIGURES</b>	<b>xv</b>
<b>LIST OF SYMBOLS / ABBREVIATIONS</b>	<b>xviii</b>
<b>CHAPTER</b>	
<b>1 INTRODUCTION</b>	<b>1</b>
1.1 Background and environmental aspect	1
1.2 Dyes	2
1.2.1 Reactive Orange 16	4
1.3 Treatments of industrial effluents	5
1.4 Adsorbent	7
1.4.1 Chitosan beads	7
1.5 Objectives	10
<b>2 LITERATURE REVIEW</b>	<b>11</b>
2.1 Adsorption	12
2.1.1 Removal of dyes	12
2.1.2 Removal of heavy metal ions	17
2.2 Chitosan-based adsorbent	20
2.2.1 Dyes removal	20
2.2.2 Heavy metal ion removal	29
2.3 Reactive Orange 16 as adsorbate	31
2.4 Comparative research	35
2.4.1 Chitosan-based adsorbent	35
2.4.2 Reactive Orange 16 as adsorbate	36

3	MATERIALS AND METHODS	37
3.1	Chemicals and reagents	37
3.2	Adsorbent preparation	38
3.3	Adsorbate preparation	38
3.4	Batch studies	39
3.4.1	Effect of contact time	40
3.4.2	Effect of initial concentration of RO16 dye	40
3.4.3	Effect of adsorbent dosage	40
3.4.4	Effect of agitation rate	40
3.4.5	Effect of pH	41
3.5	Adsorption isotherm	41
3.6	Adsorption kinetics	42
3.7	Modification of chitosan beads	42
3.7.1	Addition of polyethylene glycol (PEG)	42
3.8	Optimization studies	42
3.8.1	Plackett-Burman Design (PBD)	42
3.8.2	Optimization of percentage uptake by Response Surface Methodology (RSM) Analysis	43
3.9	Characterization Analysis	44
3.9.1	UV-Visible Spectroscopy	44
3.9.2	Attenuated Total Reflectance-Fourier Transform Infrared Spectroscopy (ATR-FTIR)	44
3.9.3	Scanning Electron Microscope (SEM)	44
3.9.4	Atomic Force Microscope (AFM)	44
4	RESULTS AND DISCUSSION	45
4.1	Characterization analysis	45
4.1.1	Attenuated Total Reflectance-Fourier Transform Infrared Spectroscopy (ATR-FTIR) analysis	45
4.1.2	Scanning Electron Microscope (SEM) analysis	49
4.1.3	Atomic Force Microscope (AFM) analysis	51
4.2	Batch studies	53

4.2.1	Effect of contact time and initial concentration of dye	53
4.2.2	Effect of adsorbent dosage	55
4.2.3	Effect of agitation rate	57
4.2.4	Effect of pH	59
4.3	Adsorption isotherm	62
4.3.1	Langmuir isotherm	62
4.3.2	Freundlich isotherm	66
4.3.3	Brunauer-Emmett-Teller (BET) isotherm	69
4.4	Adsorption kinetics studies	72
4.4.1	Pseudo-first order kinetics model	72
4.4.2	Pseudo-second order kinetics model	74
4.5	Modification of chitosan beads	81
4.5.1	Addition of polyethylene glycol (PEG)	81
4.6	Optimization studies of dye adsorption	84
4.6.1	Plackett-Burman Design (PBD)	84
4.6.2	Verification of Plackett-Burman Design models	86
4.6.3	Optimization of percentage uptake by Response Surface Methodology (RSM) Analysis	87
4.6.4	Interaction between contact time and pH on uptake removal	90
4.6.5	Verification of Response Surface Methodology (RSM) Analysis	92
5	CONCLUSION	94
5.1	Conclusion	94
5.2	Future Prospects	95
	REFERENCES	96
	APPENDICES	109

## LIST OF TABLES

<b>Table</b>		<b>Page</b>
1.2	Classification of dyes	3
2.2.1	Functional group of chitosan present in the FTIR spectrum	22
2.4.1	Adsorption of different pollutants by chitosan-based adsorbent	35
2.4.2	Adsorption of RO16 by various type of adsorbent	36
3.1	Chemicals and reagents used	37
4.1.1	Comparison of peaks before and after adsorption	49
4.3.1.1	$R_L$ values of different types of adsorption isotherms	65
4.3.1.2	$R_L$ value for the RO16 dye concentration range examined	66
4.3	Isotherms parameters and coefficient of determination in RO16 adsorption by chitosan beads	71
4.4	Comparison between pseudo-first and second order kinetics model in terms of their adsorption capacities, kinetic model parameters and correlation coefficients	78
4.6.1	Regression Analysis (ANOVA) of Plackett-Burman for the removal of RO16	85

4.6.2	Experimental conditions of PBD for adsorption of RO16 using chitosan beads, with both experimental and predicted uptake	86
4.6.3	Regression analysis (ANOVA) of RSM for RO16	89
4.6.5	Experimental conditions of RSM for adsorption of RO16 using chitosan beads, with both experimental and predicted uptake	93

## LIST OF FIGURES

<b>Figure</b>		<b>Page</b>
1.2.1	Chemical structure of RO16	4
1.2.2	Harmful impact of azo dyes to human and environment	5
1.3	Several technologies for treating wastewater containing dye	6
1.4.1	Chemical structure of chitosan	7
1.4.2	Transformation of chitin to chitosan beads	9
2.1.1	SEM images of pineapple stem (a) before and (b) after adsorption with magnification of 350×	14
2.1.2	FTIR spectrum of NTA-SB	16
2.1.3	FTIR spectrum of XOP and OP	19
2.2.1	FTIR spectrum of chitosan beads before and after RR adsorption	23
2.2.2	SEM image of chitosan	23
2.2.3	SEM of (i) chitosan before adsorption, (ii) after adsorption of AB9 and (iii) after adsorption of FY3	25
2.2.4	SEM image of chitosan beads before removal of RB5	26
2.2.5	FTIR spectrum of chitosan beads	27
2.3.1	Possible interaction between RO16 and CCTPP/TiO <sub>2</sub> NC	34
4.1.1.1	Spectrum of chitosan beads before adsorption of RO16	47
4.1.1.2	Spectrum of chitosan beads after adsorption of RO16	48
4.1.2.1	SEM image of chitosan beads before RO16 adsorption	50

4.1.2.2	SEM image of chitosan beads after RO16 adsorption	50
4.1.3.1	AFM image of chitosan beads before RO16 dye adsorption	52
4.1.3.2	AFM image of chitosan beads before RO16 dye adsorption	52
4.2.1	Effect of contact time and initial concentration of RO16 towards adsorption	54
4.2.2	Effect of dosage of chitosan beads on RO16 removal	56
4.2.3	Effect of agitation rate on adsorption of RO16 by chitosan beads	58
4.2.4	Effect of pH on the adsorption of RO16 by chitosan beads	61
4.3.1	Langmuir isotherm plot for the adsorption of RO16 onto chitosan beads	64
4.3.2	Freundlich isotherm plot for the adsorption of RO16 onto chitosan beads	68
4.3.3	BET isotherm plot for the adsorption of RO16 onto chitosan beads	70
4.4.1	Pseudo-first order plot for the adsorption of RO16 onto chitosan beads	74
4.4.2	Pseudo-second order plot for the adsorption of RO16 onto chitosan beads	77
4.4.3	Comparison between experimental and theoretical model of RO16 adsorption onto chitosan beads	80
4.5.1	Chemical structure of PEG	81



4.5.2	Comparison between uptake removal of RO16 using native chitosan beads and modified chitosan beads with PEG	83
4.6.4	3D surface plot for the uptake removal of RO16 by chitosan beads varying with pH and contact time at initial dye concentration of 100 mg/L and 0.05 g of adsorbent dosage	90

## LIST OF SYMBOLS / ABBREVIATIONS

$C_e$	Concentration of RO16 dye at equilibrium, mg/L
$C_o$	Initial RO16 concentration, mg/L
$C_S$	RO16 concentration at saturation, mg/L
$C_t$	RO16 concentration at time, mg/L
$h$	Initial adsorption rate, mg/g min
$K_B$	BET constant
$K_L$	Langmuir isotherm constant related to energy of chitosan beads, L/mg
$K_F$	Freundlich isotherm constant for adsorption capacity, mg/g
$k_1$	Pseudo-first order kinetics rate constant, min <sup>-1</sup>
$k_2$	Pseudo-second order kinetics rate constant, g/mg min
$m$	Mass of chitosan beads, g
$n$	Freundlich constant for intensity
$q_e$	Amount of RO16 dye adsorbed at equilibrium, mg/g
$q_{e,cal}$	Calculated $q_e$ value
$q_{e,exp}$	Experimental $q_e$ value
$q_m$	Maximum adsorption capacity of chitosan beads, mg/g
$q_t$	Amount of RO16 adsorbed at time t, mg/g
$R_L$	Equilibrium parameter
$t$	time, minutes
$V$	Volume of dye solution, L
AB9	Acid blue 9
AFM	Atomic Force Microscopy
ATR-FTIR	Attenuated Total Reflectance-Fourier Transform Infrared Spectroscopy
ANOVA	Analysis of variance
BB3	Basic blue 3
BET	Brunauer–Emmett–Teller
CBR	Cibacron Brilliant Red 3B-A

CBY	Cibacron Brilliant Yellow 3G-P
CCD	Central Composite Design
Cd	Cadmium
Cr	Chromium
CS	Chitosan
CTPP	Chitosan-tripolyphosphate
C-TPP-PEE	Chitosan/tripolyphosphate/mushroom green composite
Cu	Copper
C.V.	Coefficient of variation
DEO	1,2:7,8-diepoxyoctane
DR23	Direct Red 23
DR80	Direct Red 80
DY	Direct Yellow
ECH	Epichlorohydrin
EDS	Energy dispersive spectroscopy
FT-IR	Fourier Transform-Infrared Spectroscopy
FY3	Food Yellow 3
KBr	Potassium bromide
KOH	Potassium hydroxide
MB	Methylene blue
MG	Malachite Green
MKCF	Modified kenaf core fiber
MSBs	Modified sugarcane bagasses
NaOH	Sodium hydroxide
NTA-SB	Nitrilotriacetic acid modified sugarcane bagasse
ORH	Oxalic acid modified rice hull
Pb	Lead
PBD	Plackett-Burman Design
PEG	Polyethylene glycol
pH <sub>pzc</sub>	Point of zero charge
R <sup>2</sup>	Coefficient of determination
RB5	Reactive Black 5
RB10	Reactive Brown 10

RO16	Reactive Orange 16
rpm	Revolution per minutes
RR	Reactive Red
RR222	Reactive Red 222
RSM	Response Surface Methodology
SEM	Scanning Electron Microscopy
UV/Vis	Ultraviolet-Visible

## **CHAPTER 1**

### **INTRODUCTION**

#### **1.1 Background and Environmental aspects**

The dyeing of textiles has existed since the Neolithic era. Back then, most of the dyes were obtained from the natural sources such as plants and insects. In the ancient time, scarce dyestuffs such as Tyrian purple was highly valued luxury goods as it was able to provide vibrant and long lasting colour (Abel, 2012). The discovery of Mauveine, the first ever synthetic dye, by William Henry Perkin in 1856 brought about a significant revolution in dyes (Bernard, 2018). The discovery of mauveine sparked a rise in synthetic dyes and the advancement in immunology and chemotherapy. Within these few decades, synthetic dyes were accessible almost everywhere, sparking a revolution in fashion, but also having an impact on the environment.

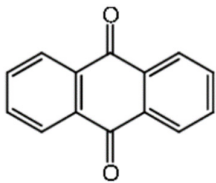
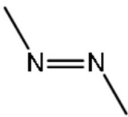
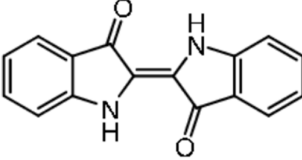
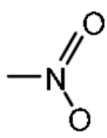
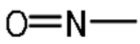
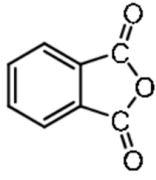
The issue of water pollution has grown increasingly complex and widespread in recent decades. With the increasing needs and demand, there are over 100,000 commercially dyes that exist and the present global dye manufacturing rate is around 800,000 tons per year (Jamee & Siddique, 2019). A major portion of the dyes produced are employed in the textile industry. According to Pourrahim et al. (2020), it is estimated that around 15% of the industrial dyes used are

discarded as wastewater. Textile industries are among the biggest producers of wastewater containing dyes since textile dyeing process is water intensive. The problem of industrial effluent containing dyes is significant as most of the dyes possessed high toxicity, mutagenicity and carcinogenicity (Gregory et al., 1991). The intense colour of wastewater that contain dyes block solar radiation from passing through, impairing photosynthesis, which then altering the aquatic biota, and causing acute and chronic damage to these ecosystems. The residual dyestuff was also linked to a number of human health concerns, including inflammation, respiratory issues, and skin diseases. The toxicity and environmental impact of dyes are of major concern. Hence, it is critical to reduce and remove organic contaminants from wastewater prior to discharge.

## **1.2 Dyes**

A dye is a colored substance that chemically bonds with the surface to which it is applied. Dyes consists of two main components which are auxochromes that determine the colour intensity of the dye, and chromophores, which determine its colour. The chromophore is made up of atom groups, most often alkenes ( $-C=C-$ ), thiocarbonyl ( $-C=S$ ), nitroso ( $-N=O$ ), carbonyl ( $-C=O$ ), azo ( $-N=N-$ ), nitro ( $-NO_2$ ) and so on. The polar auxochromes group such as hydroxyl ( $-OH$ ) and amino ( $-NH_2$ ) group make the dye soluble in water and bind to the fabric by interaction between the oppositely charged groups. Dyes can be classified into various categories by its functional groups such as azo, anthraquinone, indigo, phthalein, nitroso, nitro and so on. Table 1.2 shows the classification of dye according to their functional groups.

**Table 1.2:** Classification of dyes.

Class	Structure/Chromophore
Anthraquinone	
Azo	
Indigo	
Nitro	
Nitroso	
Phthalein	

### 1.2.1 Reactive Orange 16

Reactive Orange 16 (RO16), also referred to as Remazol Brilliant Orange 3R is a reactive azo dye that is widely used in the textile industry. Figure 1.2.1 displays the chemical structure of RO16.

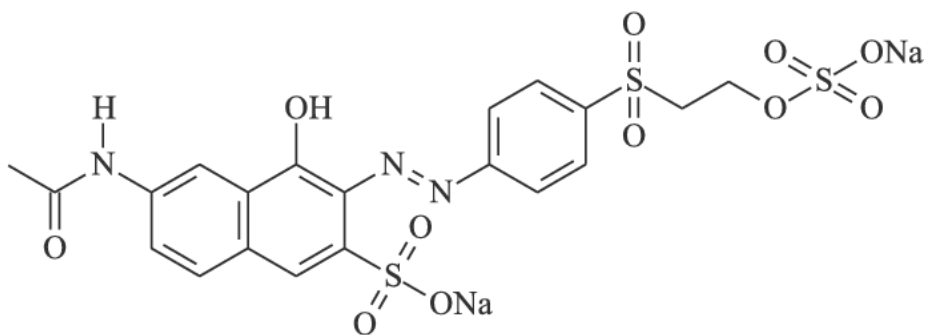


**Figure 1.2.1:** Chemical structure of RO16.

RO16 has excellent colourant characteristic such as high colour fastness to washing and light. Besides, it is also forming a strong covalent bonding with both natural and synthetic textile fibers. However, due to its high-water solubility, it can be easily absorbed by the body and can pollute the environment due to its high toxicity and mutagenic properties. The presence of complex aromatic structure of RO16 give them physicochemical thermal and optical stability, makes it difficult to be removed from water (Gunasegaran, Ravi and Shoparwe, 2020). The existence of an azo group in RO16 also reduces biodegradability and poses a concern to the environmental system. Figure 1.2.2 shows the harmful impact of azo dye to human and environment. The release of even a tiny amount of dye into water can lead to severe pollution, hence removing dyes from waste waters is a significant step.



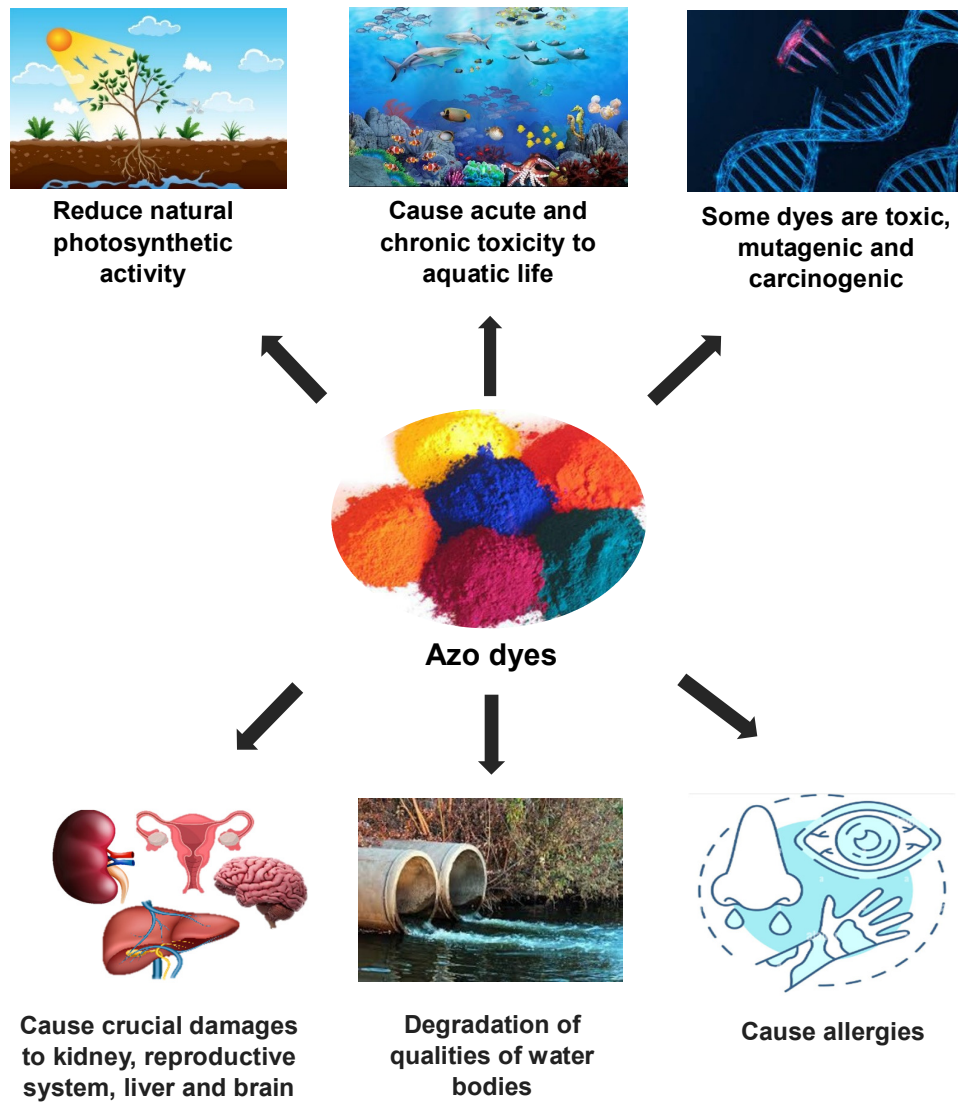


**Figure 1.2.2:** Harmful impact of azo dyes to human and environment.

### 1.3 Treatments of industrial effluents

As synthetic dyes are extremely chemically stable, persistent, and non-biodegradable, they can remain in water for an extended period of time if they are not properly treated. Electrocoagulation, ozonation, photocatalysis,

membrane filtration, ion exchange and adsorption are examples of techniques used to treat dye-containing wastewater (Senthil Kumar et al., 2019). Different dye wastewater treatment processes are depicted in Figure 1.3. Among these technologies, adsorption technique stands out as particularly efficient, having significant advantages over other approaches in terms of cost, availability, and reusability. Besides, adsorption is regarded as an environmentally friendly technique since adsorption is the process by which dye molecules are transferred from an aqueous solution to the surface of adsorbent without producing any hazardous intermediates or poisonous by-products (Jain et al., 2013).

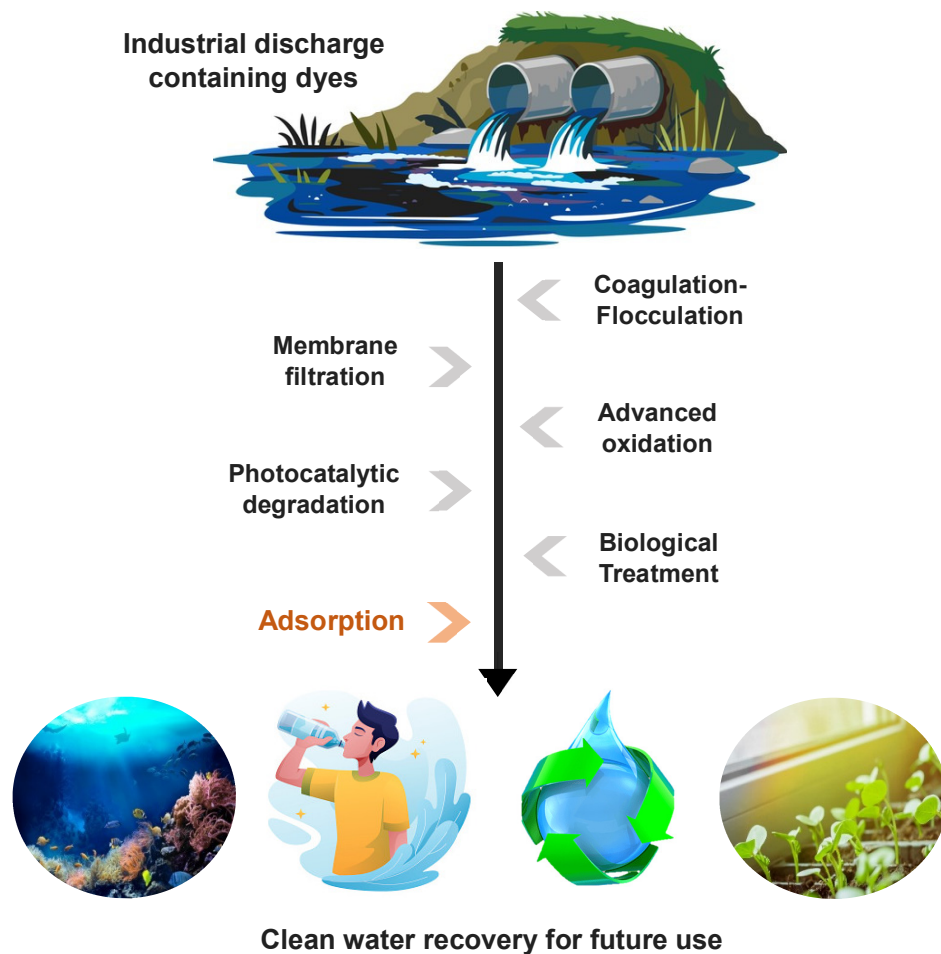


**Figure 1.3:** Several technologies for treating wastewater containing dye.

## 1.4 Adsorbent

The adsorption approach is widely used in most sectors to remove or reduce effluents. Adsorption with conventional activated carbon is considered to be one of the most successful and effective method. However, its cost of disposal has diverted the attention to the bio-based adsorbent materials including plant, animal and agricultural wastes which outperform synthetic adsorbents in the recent years. Using biobased adsorbent materials as an adsorbent is advantageous not only because it is a more cost-effective approach, but also due to its high effectiveness in removing dyes. Furthermore, the regeneration of these adsorbents is easier than that of the biomass of living organisms (Saravanan et al., 2021). It is significantly more environmentally and economically sustainable. As a result, this work focuses on the capability of chitosan beads to remove RO16 from aqueous solution.

### 1.4.1 Chitosan beads

Chitosan consists of a linear polysaccharide made up of D-glucosamine units, which are deacetylated and N-acetyl-D-glucosamine units, which are acetylated, and are randomly distributed along the chain. The chemical structure of chitosan is shown in Figure 1.4.1.

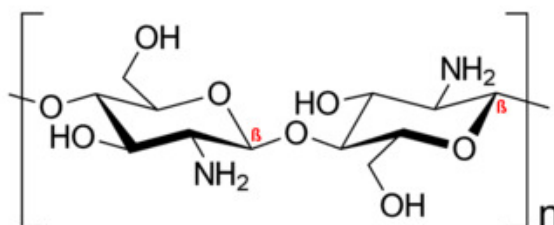


**Figure 1.4.1:** Chemical structure of chitosan.

Commercially, chitosan is derived through deacetylation of chitin, which serves as the structural material in the exoskeletons of crustaceans like shrimp, lobsters, and clams. Crustacean waste, including shells and other inedible fractions, is an underappreciated source of chitin which resulting in resource wastage. In 2020, the crustacean production has risen to 16.6 million metric tons annually, with the majority of expansion occurring in Asian countries (FAO, 2022). Crustaceans comprise roughly 40% meat, with the other 60% being inedible, prompting concerns in the industries about the extent of crustacean waste accumulation. Therefore, it is a good idea of upcycling the chitin waste into value-added commodities such as chitosan. Chitosan is one of the most abundant biosorbents found in nature and it is a cationic amino polysaccharide. It has several commercial and possible biomedical uses in the medicine, agriculture industry. The utilization of chitosan to remove dyes from wastewater has drawn a lot of attention in earlier research. In other words, chitosan is an ecofriendly and biodegradability raw materials. Apart from that, it is also easily modifiable. In this study, chitosan would be modified into beads form. Chitosan that available in the market often appears in fine powder form, therefore the purpose of transforming it into beads is to ease the after-treatment process or to avoid filtration. The production of chitosan beads in this study involves improving on previously published processes in order to make it even more cost-effective. Figure 1.4.2 shows the simple illustration of transformation of chitin into chitosan beads.



**Chitin from crustaceans waste**

↓  
**Deacetylation**



**Chitosan**



**Chitosan beads**

**Figure 1.4.2:** Transformation of chitin to chitosan beads.

## 1.5 Objectives

The goals of this research are:

1. To produce a low cost and effective adsorbent for the removal of RO16 from aqueous solution.
2. To study the adsorption performance of chitosan beads as adsorbent for RO16 removal.
3. To study the effect of several parameters such as contact time, initial RO16 adsorbate concentration, dosage of chitosan beads, agitation rate and pH towards the adsorption performance.
4. To determine the suitable adsorption isotherm model and adsorption kinetics model that describes the adsorption of RO16 onto chitosan beads.
5. To carry out the characterization studies on the adsorbent by Attenuated Total Reflectance-Fourier Transform Infrared Spectroscopy (ATR-FTIR), Scanning Electron Microscopy (SEM) and Atomic Force Microscopy (AFM).
6. To optimize the operating condition for RO16 dye removal by utilizing Plackett-Burman Design (PBD) and Response Surface Methodology (RSM).

## **CHAPTER 2**

### **LITERATURE REVIEW**

One of the most traditional and well-known methods for treating water and wastewater is adsorption. Adsorption involves the movement of a molecule from the bulk of a liquid to the surface of a solid, constituting a surface phenomenon.

The performance's of an adsorbent is greatly influenced by its surface condition which can be affected by the modification techniques used, as well as the chemical composition of the material. The characteristics of the adsorbent's surface and structure can be altered through physical and chemical modification. In general, an adsorbent with porous structure and large surface area with appropriate surface's condition can often adsorb the pollutants effectively. For example, some adsorbents when subjected to modifications such as acids, alkaline, cross-linking agent or oxidizing agent, significant improvements can be achieved in their adsorption efficiency. Modifications often aim to increase the surface areas, modify the functional groups, improve the magnetic performance and increase the catalytic capacity of the adsorbent used.

Many studies reported that adsorption is a low-cost water filtration process that can be extremely successful in eliminating some of the hazardous pollutants. The

feasibility of using agricultural waste or chitosan as the potential adsorbent to remove various types of pollutants from wastewater have been studied, summarized, and reviewed in the following part.

## **2.1 Adsorption**

### **2.1.1 Removal of dyes**

Biosorbent from agricultural and food waste such as shells of wheat, orange peels, sunflower leaves, fruit wastes were reported to be potential adsorbent, serving as a viable alternative to those costly methods used to remove dyes from solutions.

Salih, Abdul Kareem and Anwer (2022) studied the potential of raw corn cob to remove anionic dyes, methyl red and methyl orange from aqueous solution. Multiple studies were conducted to optimize factors including temperature, initial concentration of anionic dye, dosage of corn cob and contact time. It was noted that when the contact time increased, the adsorption increased as well. But an opposite trend was observed when the concentration was increased. The authors concluded that the highest dye uptake was obtained in acidic solution with pH 1 for methyl orange and pH 4 for methyl red. The percentage removal also decreases with increasing temperature. This proven that anionic dye can be adsorbed the most under acidic medium. In this study, with 2.0 g/L of the corn cob, a considerable removal of dyes happened in a relatively short time, which was in the first 100 minutes. Under this exposure time, the adsorption capacities of 3.53 and 6.09 mg/g were recorded for methyl red and methyl orange, respectively. As for the isotherm study, the experimental data fitted the Langmuir



isotherm model better than the Freundlich isotherm model. Therefore, it was concluded that methyl red and methyl orange adsorption on the unprocessed corn cob surface is homogeneous in nature.

The similar parameters were carried out by Hameed, Krishna and Sata (2009) on the study employing pineapple stem to remove cationic dye, methylene blue (MB) from aqueous solution. Based on the findings, increased in dye concentration led to higher quantity of dye adsorbed and it slowly became constant after achieving the equilibrium. The concentration gradient provides a strong driving force to overcome the dye's mass transfer resistance towards the adsorbent. Besides, as the pH was adjusted from 2 to 10, the dye uptake was increasing from 13.29 mg/g to 104.50 mg/g. This is because methylene blue is a cationic dye which exhibit a better uptake under alkaline condition. The kinetic modeling analysis revealed that the equilibrium data followed pseudo-second order model, indicating chemical adsorption. The  $R^2$  values of Freundlich isotherm and Langmuir isotherm were reported to be 0.921 and 0.998, respectively. This indicated Langmuir isotherm showed a better fit compared to Freundlich isotherm with a maximum monolayer adsorption capacity of 119.05 mg/g. In order to have a clearer picture for the adsorption of MB, SEM was performed and Figure 2.1.1 shows the SEM images of pineapple stem (a) before adsorption and (b) after adsorption of MB. It was apparent that pineapple stem contained large amount of pores and this structure offered an advantage to improve the adsorption process.

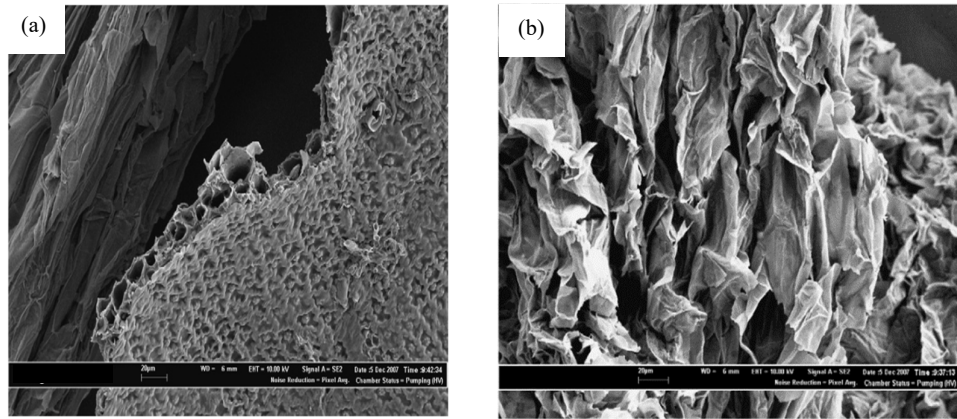


**Figure 2.1.1:** SEM images of pineapple stem (a) before and (b) after adsorption with magnification of 350 $\times$ .

In another work, Lee and Ong (2014) who focused on using oxalic acid modified rice hull (ORH) for removing MB also showed positive outcome. The adsorption studies confirmed that ORH successfully removed as high as 97% of MB in the optimum pH condition. In the comparative study, it is cleared that rice hull in its native form can remove MB. However, when dye concentrations increased, the efficiency decreased dramatically. In contrast, ORH continued to display a high percentage of uptake irrespective of the MB concentrations. The authors concluded that the introduction of  $\text{COO}^-$  functional groups onto the adsorbent during the modification process increased the number of negatively charged binding sites for positively charged MB cations, which subsequently enhanced the adsorption process. From the kinetic study, it was proven that pseudo-second order kinetics has a greater fitting than pseudo-first order as the experimental data gives a  $R^2$  of 1 and 0.9999 which is close to unity for 50 and 100 mg/L of MB, respectively. Besides, the findings demonstrated that the Langmuir isotherm described the system under study better than the Freundlich isotherm.

The highest sorption capacity of ORH was determined to be 29.15 mg/g. This has further proven that ORH can serve as a cost-effective substitute for expensive adsorbents in dye removal.

Ong et al. (2013) evaluated the effectiveness of nitrilotriacetic acid modified sugarcane bagasse (NTA-SB) to remove basic blue 3 dye (BB3). The modification of sugarcane bagasse used in this study resulted in a high adsorption capacity, 54.35 mg/g for BB3. The BB3 uptake was pH-dependent, with the optimum pH occurring in the range of pH 5 to 9 and the sorption achieved equilibrium after the first hour. Besides, the authors concluded that the observed kinetic data obeyed to pseudo-second order model, showing that chemical adsorption was the rate determining step. FTIR analysis was performed to prove the presence of important functional group in the NTA-SB. The FTIR spectrum for the peak at  $1636\text{ cm}^{-1}$  was assigned to the C=C stretching of the aromatic group in lignin and the presence of lignin in sugarcane bagasse is further shown by the significant absorption peak at  $1051\text{ cm}^{-1}$ , which revealed to be the C-O band. Figure 2.1.2 shows the FTIR spectrum of NTA-SB. The authors reported that the uptake removal of BB3 was higher by using NTA-SB than the native sugarcane bagasse. This was due to the positively charged BB3 cations appear to bind to the bagasse more easily when acetate anions were introduced during the modification process.

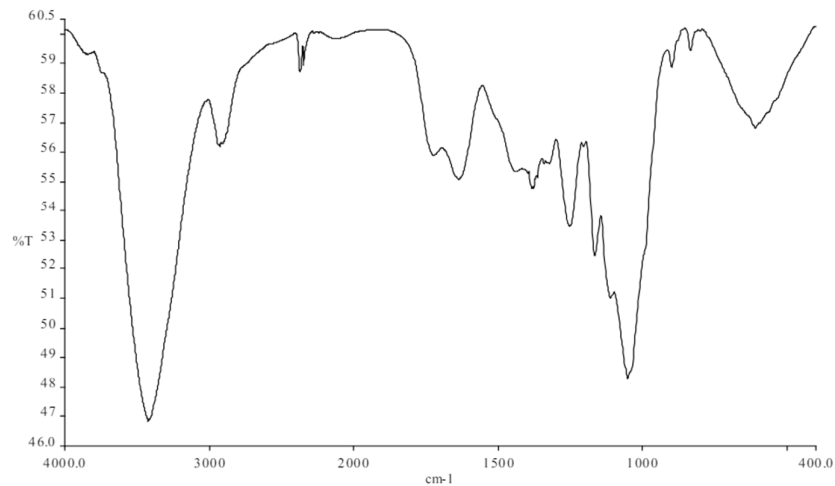


**Figure 2.1.2:** FTIR spectrum of NTA-SB.

The ability of orange peel to remove dye from sewage was studied by Arami et al. (2005). The targeted dye in their work was Direct Red 80 (DR80) and Direct Red 23 (DR23). In their study, pH 2 was determined as the best operating condition for removing both dyes with adsorption capacity of 21.05 mg/g for DR80 and 10.72 mg/g achieved for DR23. The authors also concluded that pseudo-second order and Langmuir isotherm model can be used to describe the adsorption process as evidenced by the high  $R^2$  values, which exceeding 0.998. A similar work has been done by Doulati Ardejani et al. (2007) who also focused on the adsorption of DR80 and DR23 using orange peel. It was found that the adsorption process correlates better into Langmuir isotherm model and follows pseudo-second kinetics model.

### **2.1.2 Removal of heavy metal ions**

Besides from dyes, wastewater containing heavy metal ions such as copper, zinc and lead ion also received much attention since it poses hazards to the environment and human health.

Karnitz et al. (2007) studied the capability of modified sugarcane bagasses (MSBs) to adsorb three metal ions which are  $\text{Cu}^{2+}$ ,  $\text{Cd}^{2+}$ , and  $\text{Pb}^{2+}$  ions. The sugarcane bagasses was chemically modified by introducing the carboxylic acid and amine groups onto it. This resulted MSBs showed a high adsorption ability for  $\text{Cu}^{2+}$ ,  $\text{Cd}^{2+}$ , and  $\text{Pb}^{2+}$  ions. Based on the findings, in 50 minutes of contact time, the adsorption equilibrium for all three ions was reached. Besides, as pH increases, the sorption of the metal ions increases as well.  $\text{Cd}^{2+}$  was observed to achieve the highest removal at pH 6, while  $\text{Pb}^{2+}$  and  $\text{Cu}^{2+}$  removal was the highest at pH 5 and 5.5, respectively. As for the isotherm study, the adsorption process matched more closely with the Langmuir isotherm model as a higher  $R^2$  value was obtained compared to Freundlich isotherm model. This indicated that the system was associated with monolayer adsorption.

Gupta, Kumar and Gaur (2009) evaluated the effectiveness of using coir fibers, rice stem, rice husk, banana peels, discarded tea leaves and peanut hulls in removing lead ions. It was found that the most effective sorbent for  $\text{Pb(II)}$  ions was peepul leaves with the maximum adsorption capacity of 127.34 mg/g. Grass clippings demonstrated the lowest adsorption capacity, which is only 29.05 mg/g. As for the rice husk, mango leaves, discarded tea leaves, teak saw dust, rice stem,

coir fibers, peanut hulls and banana peels, the recorded adsorption capacities were 31.13 mg/g, 31.54 mg/g, 35.89 mg/g, 40.70 mg/g, 49.57 mg/g, 52.03 mg/g, 69.75 mg/g and 72.79 mg/g, respectively. The majority of the examined plant materials were able to rapidly adsorb Pb(II) ions from solution, with more than 90% sorption happening within 10 minutes. Besides, most of the sorption of Pb(II) ions obtained highest removal at pH 4 and 5. The isotherm findings for sorption of Pb(II) ions exhibited good agreement with Langmuir isotherm models with high  $R^2$  values, between 0.96 to 0.99 compared to Freundlich model. For the kinetic study, the pseudo-second order showed a better fitness compared to pseudo-first order. The external diffusion was identified as the primary mechanism of Pb(II) ions adsorption for all the tested plant materials.

The same removal of the  $Pb^{2+}$  ions was analyzed by Liang et al. (2009) using orange peel xanthate (XOP). In their work, sulfur groups were chemically incorporated into the orange peel. Figure 2.1.3 displays the spectrum of orange peel xanthate and native orange peel. The additional new bands appeared at  $1151.3\text{ cm}^{-1}$ ,  $1019.6\text{ cm}^{-1}$  and  $538.3\text{ cm}^{-1}$  in spectrum proven the presence of sulfur groups in XOP. The adsorption process was not greatly affected by the effect of temperature and the equilibrium was achieved within 20 minutes. The kinetic study of the system conformed to the pseudo-second order model. It was found that at  $30\text{ }^\circ\text{C}$  and pH 5.0, orange peel xanthate obtained a maximum adsorption capacity of 204.50 mg/g, and this was approximately 150% more than that of native orange peel. This has proven that the modified orange peel is a much more efficient adsorbent compared to the native ones.

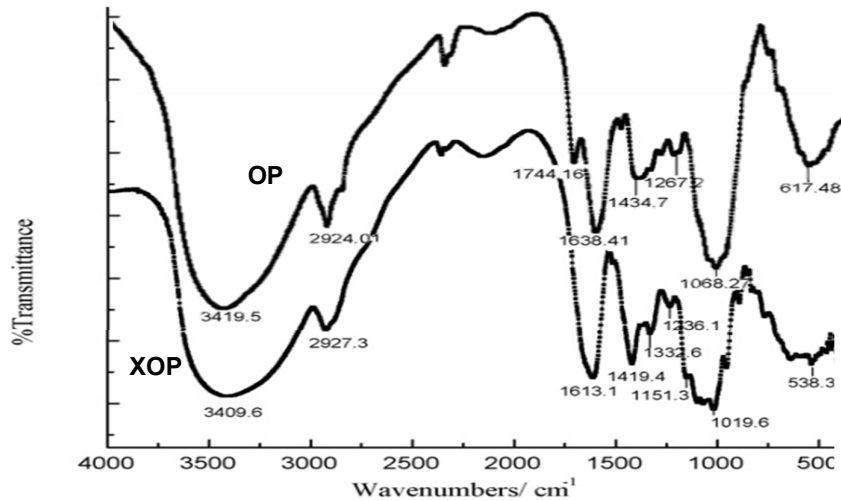


**Figure 2.1.3:** FTIR spectrum of XOP and OP.

In another work conducted by Qaiser, Saleemi and Umar (2009), the adsorption of lead using *Ficus religiosa* leaves showed promising results. The biosorption occurred spontaneously and relatively fast whereby 60 to 70% of uptake was achieved in the first 15 minutes and equilibrium was attained within 1 hour. A maximum biosorption capacity of 37.45 mg/g was recorded at pH 4 and the optimum temperature was determined to be 25°C. The models that best fit the kinetics and equilibrium of the biosorption process were determined to be the pseudo-second order and the Langmuir isotherm models, respectively.

The feasibility of using potassium hydroxide treated guava leaves as an adsorbent for zinc ions removal was investigated by Sireesha et al. (2023). The adsorption process was able to achieve equilibrium in a period of 20 minutes, at pH 3 and 100 mg/L of guava leaves. The study showed that KOH-treated guava

leaves have an adsorption capacity of 14.5 mg/g as compared to the untreated guava leaves which was only 5.1 mg/g.

Based on the above findings, agricultural wastes are believed to be having a great potential as a low cost and efficient adsorbent in the adsorption field.

## **2.2 Chitosan-based adsorbent**

In recent years, chitosan has gained popularity as a promising adsorbent material due to its unique characteristics. In view of the existence of amine and hydroxyl groups in its structure, chitosan has the capability to engage in various potential adsorption interactions with contaminants such as metals, pesticides, phenols and medicines. The adsorption capacity and polycationic characteristic of chitosan allows it to interact with other molecules efficiently and enhanced the adsorption process. In addition to these, some other outstanding qualities of chitosan, which include biodegradability, biocompatibility and antimicrobial activity also giving chitosan a great deal of potential in adsorption field. Several studies demonstrated the utilization of chitosan-based adsorbent to remove pollutants from aqueous solutions through adsorption.

### **2.2.1 Dyes removal**

Chitosan-based adsorbent can be very useful in the removal of dyes. Subramani and Thinakaran (2017) conducted a study to evaluate the usefulness of chitosan for adsorption of Direct Yellow (DY), Reactive Red (RR) and Malachite Green



(MG) dyes. In order to evaluate the performance of dye removal by chitosan, the study was performed under different parameters which included pH, adsorbent dosage, temperature, interaction period and starting concentration of dye. The adsorption capacity for each dye were recorded as 250 mg/g, 1250 mg/g and 166 mg/g for DY, RR and MG, respectively. The authors concluded that raising the adsorbent dosage enhances the percentage of dye removal while decreasing the adsorption capacity.

The maximum uptake of dye was achieved at pH 5 for DY, pH 4 for RR and pH 8 for MG. Both DY and RR are anionic dye whereas MG is cationic dye. Based on their findings, the chitosan had a  $\text{pH}_{\text{pzc}}$  value of 6.7 and when the pH values were below the  $\text{pH}_{\text{pzc}}$ , the chitosan carried positive charge. Therefore, the positively charged chitosan with both negatively charged DY and RR dye would experience a significant coulombic attraction at low pH. However, when the deprotonation of sorbent occurred at pH values greater than the  $\text{pH}_{\text{pzc}}$  values, there is lesser attractive forces leading to repulsion and lower adsorption. For this reason, MG has relatively poor adsorption onto chitosan at acidic pH values because MG undergo repulsion with the positively charged adsorbent due to its cationic properties. These findings demonstrated that electrostatic interactions between the chitosan and dye molecules are essentially important in the adsorption mechanism.

Different isotherm models, namely Langmuir, Freundlich, Temkin and Redlich-Peterson were used in modelling the adsorption data and the results indicated that the data was best fitted by Langmuir isotherm, with an  $R^2$  value exceeding 0.99. The study also indicated that the pseudo-second order kinetic process aptly

described the adsorption system, with intra-particle diffusion serving as the rate-determining step. Besides, dye adsorption onto chitosan as demonstrated under the thermodynamic analysis shown that it is a viable, spontaneous and exothermic process.

FTIR spectroscopy analysis was used to confirm the existence of functional groups on chitosan adsorbent surface. The spectra of chitosan were presented in Figure 2.2.1 and the significant functional group of chitosan detected in the FTIR spectrum was summarized in Table 2.2.1.

**Table 2.2.1:** Functional group of chitosan present in the FTIR spectrum.

Type of vibration	Observed frequency (cm <sup>-1</sup> )
-OH and -NH stretching vibration (overlap)	3500-3200
C-H symmetric and asymmetric stretching vibration	2879
Primary amine group and N-H bending vibration	1680-1480
C-O stretching	1370
-CH <sub>2</sub> and -CH <sub>3</sub> bending vibration	1421 and 1320

The presence of polar functional groups on the surface of chitosan suggested that the adsorbent was able to have a high anion exchange capacity. Through comparison, there were some peak shifting observed after the adsorption. This suggested that the functional group of chitosan were involved in the reaction and

the adsorption process in removing dyes. The SEM image shown in Figure 2.2.2 indicated that chitosan possessed a long thin crystal structure on a smooth surface, which increased the likelihood of adsorbate molecules being adsorbed onto the surface. Therefore, the results have proven that the chitosan is a proficient adsorbent for eliminating dyes from wastewater.

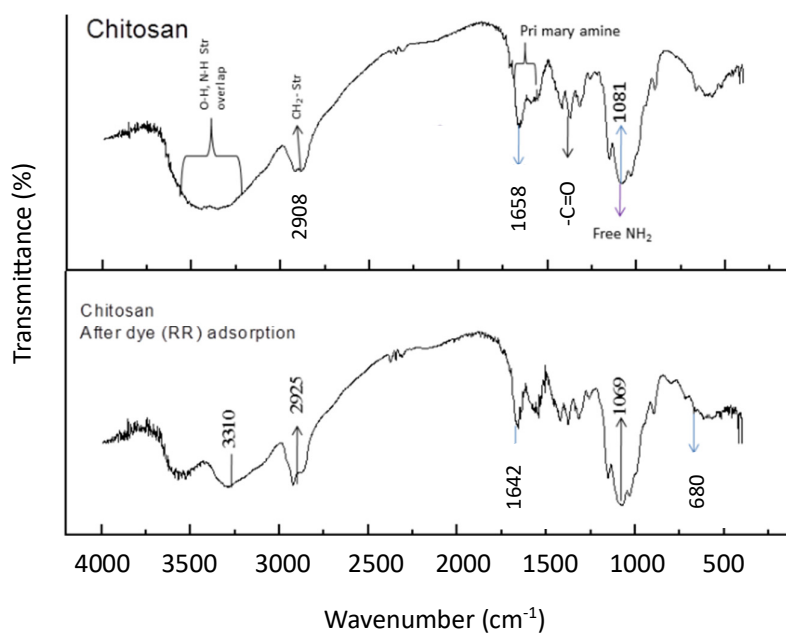


**Figure 2.2.1:** FTIR spectrum of chitosan before and after RR adsorption.

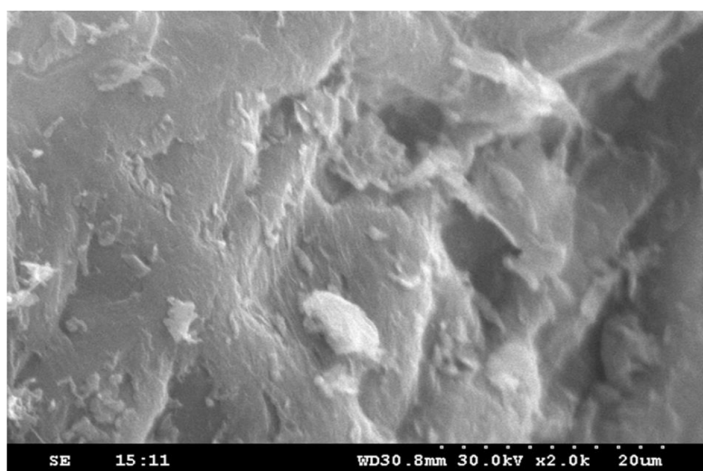


**Figure 2.2.2:** SEM image of chitosan.

Similar study on the removal of dyes by chitosan was conducted by Dotto and Pinto (2011). It was found that the optimum conditions were at 60 minutes, 150 rpm and pH 3 for removal of Acid blue 9 (AB9), whereas for Food yellow 3 (FY3), it adsorbed optimally at 60 minutes, 50 rpm and pH 3. The authors reported the maximum adsorption capacities of 295 mg/g for FY3 and 210 mg/g for AB9 under these conditions. The maximum dye uptake occurred under acidic condition and this is in accordance with the results in the study of Cheung, Szeto and McKay (2009), involving the adsorption of FY3 and AB9 by chitosan nanoparticles. Both the protonated amino groups in chitosan with FY3 and AB9 sulfonated groups interacted electrostatically leading to the adsorption process. Besides, Elovich kinetic model outperformed other models in representing experimental data with  $R^2$  value of more than 0.99. This suggested that adsorption happened via chemisorption and that food dyes were adsorbed onto the chitosan surface.

FTIR analysis identified peaks at  $2933\text{ cm}^{-1}$  which was due to the N-H stretching, and C-N stretching was seen at  $1020\text{ cm}^{-1}$  and  $1080\text{ cm}^{-1}$ . The peak at  $1640\text{ cm}^{-1}$  was corresponding to the amide I band and  $\text{-NH}_2$  band at  $1556\text{ cm}^{-1}$ . The authors concluded that these peaks match the amine's functional group on the chitosan polymer. SEM and EDS analysis also revealed the extent of coverage of chitosan surface and interactions between the chitosan's amino group and dyes' sulphonate group. Figure 2.2.3 displays the SEM of (i) chitosan before adsorption, (ii) after adsorption of AB9 and (iii) after adsorption of FY3. Before adsorption, it was revealed that the surface of chitosan was found to have a polymeric network with an uneven porous internal structure. It was observed that

the pores were no longer evident and the dyes had covered and adhered to the chitosan surface homogeneously after the adsorption of both dyes.

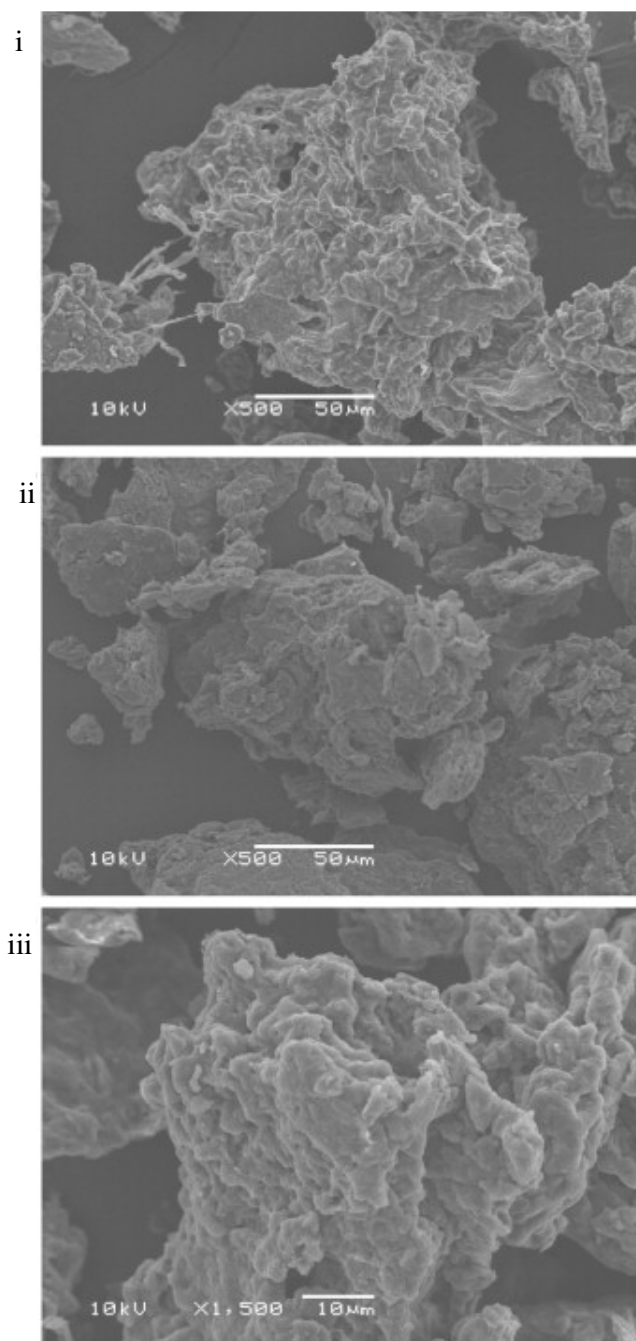


**Figure 2.2.3:** SEM of (i) chitosan before adsorption, (ii) after adsorption of AB9 and (iii) after adsorption of FY3.

In another work, chitosan was modified into beads form by Ong and Seou (2013) in order to remove reactive dye which is the Reactive Black 5 (RB5) from wastewater. They concluded that the chitosan beads performed optimally at RB5 concentration of 60 mg/L, 182.5 minutes, agitation rate of 200 rpm and pH 6. In addition, the adsorption system fitted well into the pseudo-second order kinetic model and this suggested the occurrence of chemisorption. The adsorption process obeyed to both Langmuir and BET isotherms. The surface morphology of the chitosan beads was analyzed using SEM and it was found that chitosan beads have a non-porous configuration as there was absence of cavities in the micrograph (Figure 2.2.4). Despite this, the adsorbent still showed an outstanding adsorption performance as a high percentage uptake of RB5 (96.22%) can be obtained when the operating parameters were set to their optimum values.

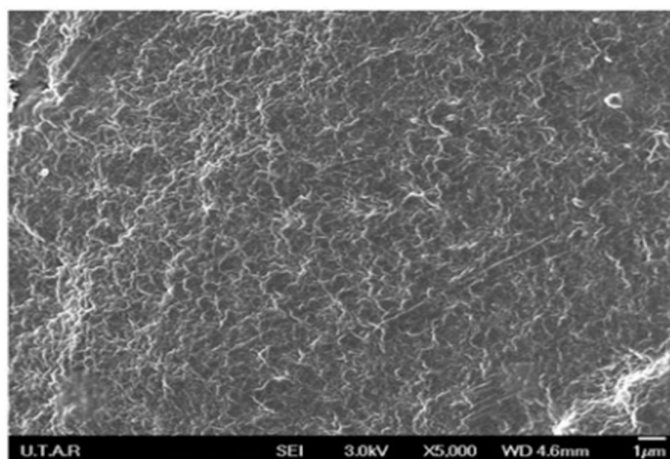


**Figure 2.2.4:** SEM of chitosan beads before removal of RB5.

Chung and Ong (2021) studied on the adsorption of Reactive Brown 10 (RB10) by chitosan beads and the findings deduced that chitosan beads were non-porous

material by referring to the SEM micrograph. The surface of native chitosan beads exhibited a wrinkled polymeric network, mirroring the morphology of cellulose due to chitosan's composition as a linear homopolymer of glucose. In addition, the results reported that the uptake efficiency was strongly pH-dependent, with a pH range of 4 to 6 being regarded as the ideal. It was discovered that 0.04 g of the chitosan beads was the optimum dosage required to remove RB10. FTIR spectrum as shown in Figure 2.2.5 also indicated the presence of  $\text{NH}_2$  and this is considered the significant functional group responsible for RB 10 adsorption.

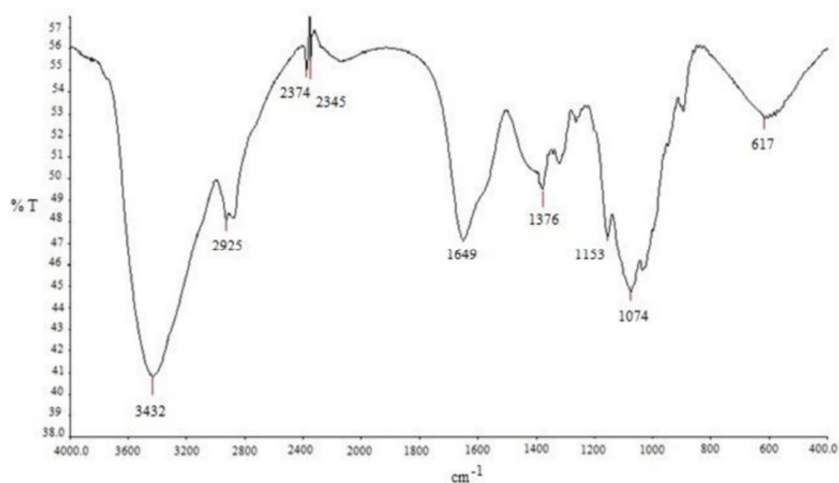


**Figure 2.2.5:** FTIR spectrum of chitosan beads.

Besides using the native chitosan beads, many researchers have modified chitosan to enhance its adsorption capabilities. One notable study was performed by Razmi et al. (2017) using modified chitosan-pandan sorbent on the adsorption of Reactive black 5 (RB5). The authors successfully used 0.2 g/L initial RB5 concentration, 0.1 g of modified chitosan-pandan and pH 7 at room temperature to obtain optimum adsorption of 99.9% in only 30 minutes. FTIR analysis for

both chitosan, the raw and the modified one, showed absorption band of 3311  $\text{cm}^{-1}$  and 3325  $\text{cm}^{-1}$ , attributed to N-H band. By comparing with the raw chitosan, the modified one showed a much more intense peak and this could be due to the modified chitosan is having more N-H groups on its surface. This subsequently led to a two-fold increase in the percentage removal of dye as compared to the raw chitosan. Hence, this has further proven that amino group played an important role in adsorption by chitosan.

The potential of employing Epichlorohydrin (ECH) bead-type cross-linked chitosan to remove the Reactive Red 222 (RR222) from wastewater was evaluated by Chiou, Kuo and Li (2003). ECH was chosen as the agent for cross-linking as it preserves chitosan's cationic amine function, which attracts anion dyes during adsorption. Additionally, it may stabilize the chitosan in acidic solutions. Initial dye concentration and pH factors were shown to have a substantial effect on adsorption capacity. The adsorption capacity rise as the starting RR222 dye concentration experienced an increment, whereas an acidic pH is advantageous for reactive dye adsorption. The RR222 equilibrium adsorption fitted well into the Langmuir model, with  $R^2$  value that was close to unity. The pseudo-second order kinetic model could be used to describe the RR222 removal using ECH cross-linked chitosan beads. The findings also revealed that at pH 3 and 30°C, the highest monolayer adsorption capacity obtained was extraordinarily high, which was up to 2252 g/kg.



Another significant study using modified chitosan beads as adsorbent was from Golfer Muedas-Taipe et al. (2020). In their work, they investigated the adsorption performance of magnetized/ethylenediamine-modified chitosan beads in the removal of azo dyes. In most cases, crosslinking is required to improve chitosan's chemical stability in acidic environments by introducing amine groups that facilitate interconnection with the azo dyes. By applying magnetic fields after adsorption, this was intended to facilitate a simple separation from the aqueous solution. It was found that at pH 2, Cibacron Brilliant Red 3B-A (CBR) was able to achieve the maximum adsorption capacity up to 377.60 mg/g whereas 179.45 mg/g was obtained in Cibacron Brilliant Yellow 3G-P (CBY). Both azo dyes adsorption conformed to the pseudo-second order kinetic model and CBY displayed a strong agreement with Langmuir isotherm model, while CBR's removal obeyed the Freundlich isotherm model better.

### **2.2.2 Heavy metal ion removal**

Vakili et al. (2018) investigated on the effectiveness of crosslinked chitosan in the adsorption of hexavalent chromium. Chitosan beads (CS) were successfully crosslinked using a water-soluble diepoxy compound [1,2:7,8-diepoxyoctane (DEO)] to improve its acid resistance. Chitosan beads were able to adsorb more Cr(VI) and remained more stable under acidic conditions after the crosslinking process. The maximum enhancement in the removal was achieved when the optimum cross-linking conditions were employed, which involved 6 g/L of DEO for 5 hours, at 50 °C and pH 10. The authors reported that CS-DEO beads at pH

2 demonstrated a remarkable maximum adsorption capacity of 325.2 mg/g compared to other crosslinked chitosan documented in the study by Bhatt, Sreedhar and Padmaja (2015) which only showed capacity of 192.3 mg/g. The experimental data obtained from CS-DEO beads was well-supported by Freundlich isotherm and pseudo-second order models.

On the other hand, Ngah and Fatinathan (2010) utilized chitosan-tripolyphosphate (CTPP) beads for the elimination of Cu(II) and Pb(II) ions. The evaluation was determined based on different parameters which were dosage of adsorbent, agitation period and pH. The pH at which Cu(II) and Pb(II) ions adsorb best was discovered at pH 4.5 and it took 0.20 g CTPP beads and 100 minutes of contact time to reach equilibrium. The maximum adsorption capacities for Cu(II) and Pb(II) ions based on the Langmuir isotherm model were 26.06 mg/g and 57.33 mg/g, respectively. Under this work, elimination of Cu(II) and Pb(II) ions both complied with the intraparticle diffusion model and pseudo-second order kinetic model. Adsorption process was observed to be spontaneous and endothermic by thermodynamic studies. Besides, according to FTIR analysis, the oxygen and nitrogen atoms present in the CTPP can serve as metal ion binding sites which explained why CTPP beads can be utilized in treating wastewater containing Cu(II) and Pb(II) ions.

Bassi, Prasher and Simpson (2000) revealed that the type of metal ion, mass of adsorbent, pH, reaction time and initial metal ion concentration exerted a notable influence on the adsorption by chitosan flakes. Among all the investigated metal

ions, Cu(II) ion exhibited the highest adsorption by chitosan. The authors found that chitosan flakes adsorbed metal ions most efficiently at pH 6.0 and 7.0. The time where equilibrium attained for the adsorption of metal ion was observed to be 3 hours and there seemed to be no change in the sorption capacity when the chitosan and metal ion mixture were shaken and not shaken. Other than that, equilibrium isotherm studies suggested that metal ion sorption onto chitosan may be represented using Langmuir isotherm model.

Thus, chitosan despite of modified or unmodified could be used as potential adsorbent as it produces efficacious results on removal of heavy metal ions and dye molecules, evident from previous studies.

### **2.3 Reactive Orange 16 as adsorbate**

Yildirim (2021) evaluated the removal of Reactive Orange 16 (RO16) by using chitosan/tripolyphosphate/mushroom green composite (C-TPP-PEE) as the adsorbent. The author conducted batch experiment and concluded that C-TPP-PEE performed optimally at 45°C, pH 5 and able to attain equilibrium in only 30 minutes. Based on experimental kinetic data at equilibrium, the pseudo-second order kinetic model fitted the data the best. Additionally, the Langmuir model exhibited the strongest correlation according to the findings, and a maximum adsorption capacity of 1001 mg/g was obtained. FTIR analysis also supported the fact that the C-TTP-PEE surface which contained the -CO, -NH, and -OH groups were important functional groups that involved in the adsorption process of RO16. For the biosorption mechanism, it was suggested that pH and

functional groups on surface of sorbent had a significant impact on the hydrogen bonding and electrostatic interactions when dealing with the removal of anionic RO16 dye.

Another notably study using RO16 as adsorbate was carried out by Abdulhameed, Mohammad and Jawad (2019). In their research, they synthesized the crosslinked chitosan-tripolyphosphate/TiO<sub>2</sub> nanocomposite (CCTPP/TiO<sub>2</sub> NC) in order to determine the RO16 removal efficiency. The highest percentage removal of 92.7% was obtained under the optimum conditions. The interaction effects between dosage of adsorbent with loading of TiO<sub>2</sub> nanoparticles into CCTPP polymeric matrix and between loading of TiO<sub>2</sub> nanoparticles into CCTPP polymeric matrix with pH were considered significant. Assembling the findings from aforementioned studies, it is cleared that chitosan may be an ideal adsorbent since there were significant interaction between chitosan and dye molecules. This study also suggested that electrostatic attraction, Yoshida H-bonding, n- $\pi$  stacking interactions and dipole-dipole hydrogen bonding interactions were involved in the adsorption mechanism, as shown in Figure 2.3.1. This was further proven by the sorption kinetics studies in which they were effectively represented by the pseudo-second order kinetic model. Hence, it was showed that functional groups on chitosan played an important role in the removal of pollutants. A maximum adsorption capacity of 618.7 mg/g was obtained and this corresponds to a 3 times increase compared to the work performed by Malakootian and Heidari (2018) who used psyllium seed powder as adsorbent to remove the same adsorbate.

In another research study, Obaid et al. (2016) studied the feasibility of using modified kenaf core fiber (MKCF) as low-cost adsorbents for the elimination of RO16. (3-chloro-2-hydroxypropyl) trimethylammonium chloride (CHMAC) was utilized as a quaternization agent on kenaf core fiber in this study. The highest RO16 removal was found to be 97.25% at 150 rpm of agitation speed, pH 6.5, at 30°C and MKCF dosage of 0.1 g/100 mL. Additionally, this adsorption system obeys to Freundlich isotherm, resulting in a multilayer adsorption capacity of 416.86 mg/g.

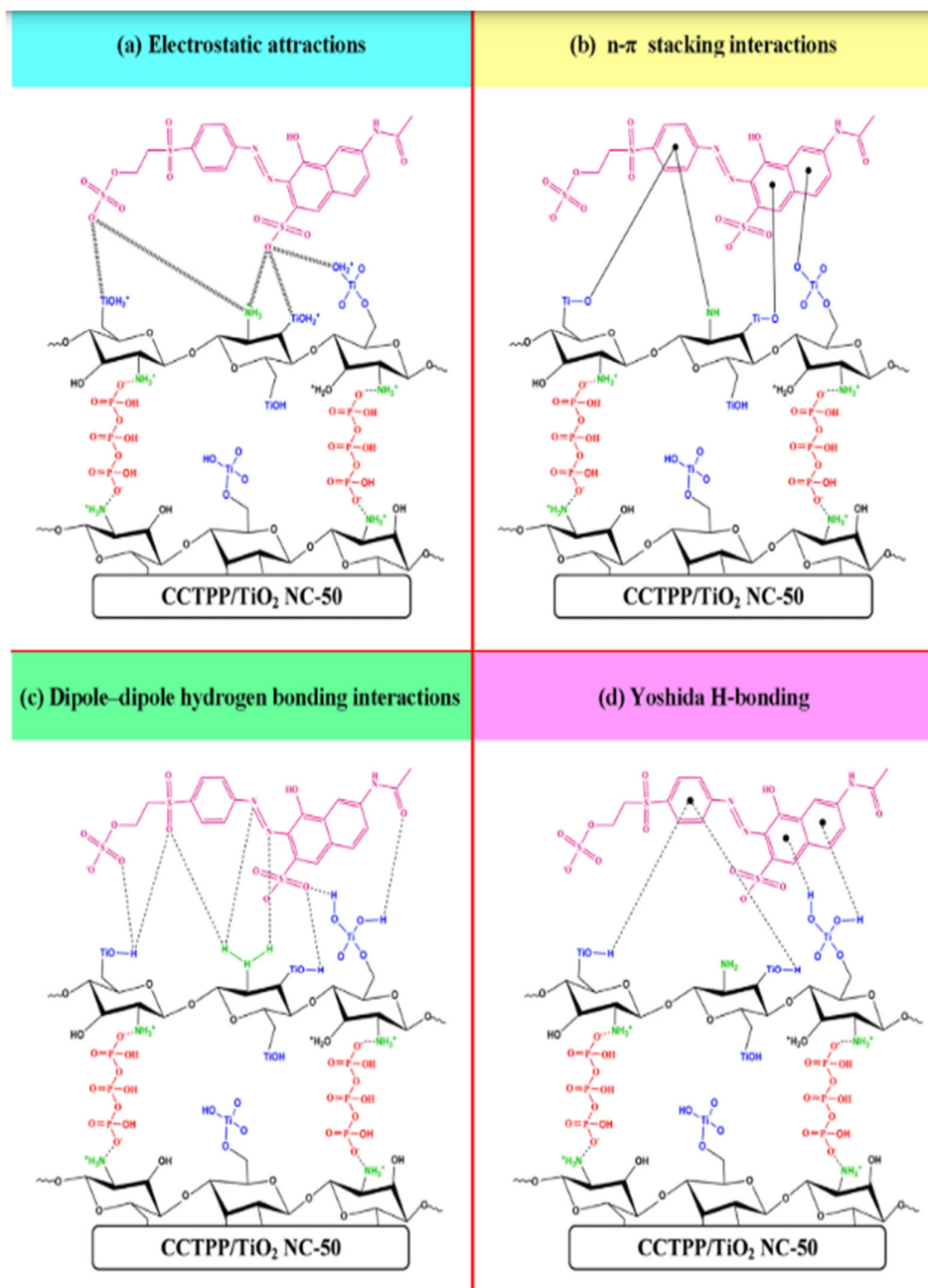


**Figure 2.3.2:** Possible interactions between RO16 and CCTPP/TiO<sub>2</sub> NC.

## 2.4 Comparative research

### 2.4.1 Chitosan-based adsorbent

**Table 2.4.1:** Adsorption of different pollutants by chitosan-based adsorbent.

Adsorbent	Adsorbate	Maximum adsorption capacity (mg/g)	References
Chitosan	Malachite Green	166.00	(Subramani and Thinakaran, 2017)
	Reactive Red	1250.00	
	Direct Yellow	250.00	
Chitosan	Acid blue 9	210.00	(Dotto and Pinto, 2011)
	Food yellow 3	295.00	
Chitosan beads	Reactive Brown 10	22.00	(Chung and Ong, 2021)
Chitosan hydrobeads	Congo red	93.00	(Chatterjee et al., 2007)
Chitosan-glyoxal/ TiO <sub>2</sub> nanocomposite	Reactive Orange 16	390.50	(Abdulhameed et al., 2019)
Magnetized/ethylenediamine-modified chitosan beads	Cibacron Brilliant Yellow 3G-P	179.45	(Golfer Muedas-Taipe et al., 2020)
	Cibacron Brilliant Red 3B-A	377.60	
Cross-linked chitosan beads with epichlorohydrin	Reactive Blue 15	722.00	Chiou and Chuang (2006)
Chitosan cross-linked with Diethylenetriaminepentaacetic acid	Chromium ion	192.30	(Bhatt, Sreedhar and Padmaja, 2015)
Chitosan-tripolyphosphate beads	Lead ion	57.33	(Nghah and Fatinathan, 2010)
	Copper ion	26.06	

#### 2.4.2 RO16 as adsorbate

**Table 2.4.2:** Adsorption of RO16 by various type of adsorbent.

Adsorbent	Maximum adsorption capacity (mg/g)	References
Chitosan/tripolyphosphate/mushroom green composite (C-TPP-PEE)	1001.00	(Yildirim, 2021)
Psyllium seed powder	206.60	(Malakootian and Heidari, 2018)
Modified kenaf core fiber	416.86	(Obaid et al., 2016)
Sunflower seed shell	22.10	(Suteu, Zaharia and Malutan, 2011)
Carbonized fish scale	105.80	(Marrakchi et al., 2017)
Rice husk ash	13.32	(Ali et al., 2018)

In summary, the research discussed above leads to the conclusion that chitosan has the potential to be an effective adsorbent for removing various pollutants from wastewater. Chitosan alone is regarded as a good adsorbent however, it is suffering from some limitations such as low solubility in acidic solutions, limited porosity and low surface area. Therefore, modification such as by incorporating it with a crosslinking agent, grafting reagent and so on can be a solution to overcome these problems. Despite the modification, the chitosan beads still possess the essential surface functional groups which are the amine and hydroxyl group that can aid in the adsorption process.



## CHAPTER 3

### MATERIALS AND METHODS

#### 3.1 Chemicals and Reagents

Table 3.1 shows all the chemicals and reagents used throughout the project.

**Table 3.1:** Chemicals and reagents used.

Chemicals/Reagents	Assay	Manufacturer
Acetic acid	99.8% (glacial)	HmbG Chemicals
Chitosan (coarse ground flakes and powder)	>75% deacetylated	Sigma Aldrich
Concentrated hydrochloric acid	37%	AnalaR NORMAPUR
Polyethylene glycol 4000	-	Merck KGaA
Reactive Orange 16 dye	Dye content $\geq 70\%$	Sigma Aldrich
Sodium hydroxide pellets	$\geq 99\%$	Merck KGaA

### **3.3 Adsorbate preparation**

Reactive Orange 16 (RO16) was utilized as adsorbate in this project. RO16 used throughout this project was purchased from Sigma Aldrich and used without any purification. RO16 has a molecular formula of  $C_{20}H_{17}N_3Na_2O_{11}S_3$  with 617.54 g/mol of molecular weight. A stock solution with the concentration of 1000 mg/L was prepared and kept in dark to prevent light degradation. Dilution was performed as needed to achieve the desired concentration in each experiment.

### **3.4 Batch studies**

In each batch experiment, 20 mL of 100 mg/L RO 16 dye solution were added with 0.05 g of chitosan beads in a 50 mL centrifuge tube. The solution was placed on the orbital shaker at the speed of 150 rpm at room temperature for 6 hours unless otherwise specified. All trials were performed in duplicates, with the average results being reported. Control studies were also conducted without the chitosan beads to confirm that the adsorption occurred was due to the chitosan beads itself and not the container walls. The supernatant of the dye solution was then being analyzed for its absorbance using UV-visible spectrophotometer, model Thermo Scientific GENESYS 50 after achieving the specified contact time. The absorbance of all the samples were measured at the wavelength of 494 nm, where maximum absorption takes place. The initial and final concentration of RO16 solution were calculated from the equation generated from calibration curve which is shown in Appendix A. After obtaining the concentration of dye solution, the percentage removal of RO16 was calculated, referring to following equation:

$$\text{Percentage removal of dye} = \frac{C_o - C_t}{C_o} \times 100\%$$

where  $C_o$  = initial RO16 concentration (mg/L),

$C_t$  = RO16 concentration at time, t (mg/L)

#### **3.4.1 Effect of contact time**

The impact of contact time was studied by adding 0.05 g of chitosan beads into 20 mL of three concentrations of RO16 which were 25 mg/L, 50 mg/L and 100 mg/L. The mixture was agitated at 150 rpm at different time intervals which were 5, 30, 60, 120, 150, 180, 240, 300 and 360 minutes.

#### **3.4.2 Effect of initial concentration of RO16 dye**

A stock solution of RO16 at a concentration of 1000 mg/L was diluted to prepare three distinct concentrations which were 25 mg/L, 50 mg/L and 100 mg/L. Similarly, 0.05 g of chitosan beads was added to each 20 mL of RO16 solution in centrifuge tube and withdrawn from orbital shaker at certain time intervals.

#### **3.4.3 Effect of adsorbent dosage**

The dosage of chitosan beads on RO16 adsorption was evaluated by adding different amounts of chitosan beads which were 0.025, 0.05, 0.075 and 0.10 g into 100 mg/L of RO16 solution. The mixtures were subjected to agitation rate at 150 rpm for 6 hours.

#### **3.4.4 Effect of agitation rate**

The impact of varying agitation rates towards adsorption of RO16 was carried out using different speeds of orbital shaker which were 100, 150 and 200 rpm. The other parameters which were concentration of dye solution, dosage of chitosan beads and contact time were kept constant at 100 mg/L, 0.05 g and 6 hours, respectively.

#### **3.4.5 Effect of pH**

In order to investigate the effect of pH, RO16 dye solutions with varying pH values ranging from pH 3 to 10 were prepared by dropwise addition of hydrochloric acid and sodium hydroxide solution of different concentration such as 0.01 M, 0.05 M and 0.10 M, prior to the experiment. A 0.05 g of chitosan beads was added to 20 mL of 100 mg/L RO16 solution with different pH and agitated for 6 hours at the speed of 150 rpm. The absorbance of the supernatant solution was then being measured by UV/Vis spectrophotometer.

#### **3.5 Adsorption isotherm**

The adsorption isotherm was examined by adding 0.05 g of chitosan beads into different concentrations of RO16 dye solution at 25, 50, 75, 100, 125, 150, 175 and 200 mg/L. The agitation rate and contact time was fixed at 150 rpm and 6 hours, respectively. The absorbance of each supernatant solution was then measured using UV/Vis spectrophotometer at 494 nm. Langmuir, Freundlich and

Brunauer–Emmett–Teller (BET) isotherms were then employed to predict the adsorption behavior.

### **3.6 Adsorption kinetics**

The adsorption kinetics were examined with initial RO16 dye concentrations of 25 mg/L and 100 mg/L. Each concentration of RO16 was added with 0.05 g of chitosan beads and shaken for different time intervals at 150 rpm. The experimental data were assessed with pseudo-first and pseudo-second order kinetic models.

### **3.9 Characterization Analysis**

#### **3.9.1 UV-Visible Spectroscopy**

After the adsorption at certain time intervals, the absorbance of the supernatant of RO16 solution were determined by the UV/Vis spectrophotometer, model Thermo Scientific GENESYS 50 at the wavelength of 494 nm.

#### **3.9.2 Attenuated Total Reflectance-Fourier Transform Infrared Spectroscopy (ATR-FTIR)**

The presence of functional groups on the chitosan beads before and after the adsorption of RO16 was determined using the Attenuated Total Reflectance (ATR), model Spectrum 2 by Perkin Elmer at the wavenumber range of 4000 to 400  $\text{cm}^{-1}$ . The chitosan beads before and after the adsorption of dye was crushed

into powder form and mixed with the KBr powder. This mixture was then ground and compressed into pellet to be analyzed.

### **3.9.3 Scanning Electron Microscope (SEM)**

The surface morphology of chitosan beads before and after the adsorption of dye was studied and analyzed using SEM model JEOL-JSM-6701 F which was operated at an emission current of 4.0 kV.

### **3.9.4 Atomic Force Microscope (AFM)**

The surface topography of chitosan beads before and after the adsorption of dye was analyzed using AFM model Park XE-70 AFM.

## CHAPTER 4

### RESULTS AND DISCUSSION

#### 4.1 Characterization analysis

##### 4.1.1 Attenuated Total Reflectance-Fourier Transform Infrared Spectroscopy (ATR-FTIR) analysis

Attenuated Total Reflectance-Fourier Transform Infrared Spectroscopy (ATR-FTIR) analysis was utilized to identify the functional group present on the chitosan beads that were involved in the adsorption process. Figures 4.1.1.1 and 4.1.1.2 reveal the spectrum of chitosan beads before and after the adsorption of RO16, respectively. Chitosan is a natural polysaccharide composed of glucosamine monomers connected through  $\beta$ -1,4 glycosidic linkage. A few important functional groups were observed in each spectrum. Based on the spectra, the significant peak at  $3452\text{ cm}^{-1}$  was attributed to the -OH and -NH stretching vibration. This band observed in the spectra was considered to be the result of the -OH and -NH stretching being overlapped with one another. The same phenomenon was observed by Vijayalakshmi (2016) and Subramani and Thinakaran (2017) who utilized chitosan as adsorbent in their studies. On top of that, the absorption peak at  $2927\text{ cm}^{-1}$  and  $2873\text{ cm}^{-1}$  corresponds to the aliphatic -CH symmetric and asymmetric stretching vibration, respectively. There was also a peak at  $1639\text{ cm}^{-1}$  denoting the presence of C=O stretching vibration. The appearance of C-N stretching was confirmed by the band at  $1381\text{ cm}^{-1}$ . Not only

these, the absorption peak at  $1155\text{ cm}^{-1}$  may denote the asymmetric stretching of the C-O-C bridge (Fernandes Queiroz et al., 2014). For peak shown at  $1074\text{ cm}^{-1}$ , it was belonged to the stretching vibration of C-O functional groups. Based on the spectrum, it can be shown that the significant functional group of chitosan was all found in the spectrum, in agreement with those previously published works.

By comparing both spectra, it was discovered that the presence of the functional group in the spectrum does not differ significantly. This could be attributed to constraints in the sensitivity of the instrument. Furthermore, it is reasonable that the spectra exhibit minimal variations and resemble each other since adsorption, which is a surface chemistry process, is mostly responsible for the dye removal process (Tay and Ong, 2019). It was found that peak shifting was observed for some absorption bands. The bands observed at  $3452\text{ cm}^{-1}$ ,  $2873\text{ cm}^{-1}$ ,  $1639\text{ cm}^{-1}$  and  $1381\text{ cm}^{-1}$  before adsorption experienced a slight shifting to  $3453\text{ cm}^{-1}$ ,  $2864\text{ cm}^{-1}$ ,  $1638\text{ cm}^{-1}$  and  $1382\text{ cm}^{-1}$ , respectively after the adsorption of RO16 (Table 4.1.1). These indicated that they are the important functional groups which participated in the binding and involved in the adsorption of RO16 by the chitosan. Slight peak shifting phenomenon was also seen in the published adsorption studies such as in Abdeen and G. Mohammad (2014), Tarik Ainane et al. (2014), Ong, Ong and Hung (2013) and Yildirim (2021).



## **4.2 Batch studies**

### **4.2.1 Effect of contact time and initial concentration of dye**

Figure 4.2.1 shows the effect of contact time and initial concentration of RO16 towards adsorption. According to the figure, it was evident that a longer contact time resulted in a higher amount of dye uptake. The amount of dye uptake was observed to be increased gradually from the beginning and started to have a significant increase after 120 minutes. The amount of dye uptake was then slowed down and attained equilibrium at 360 minutes. There was only a minimal difference in the amount of dye uptake at 360 minutes and 480 minutes. During the initial stage of the adsorption process, the rise in the dye uptake was closely associated with the large availability of free active site on the chitosan beads which enabled for the binding of RO16 molecules. It was proposed that the dye molecules and the adsorbent were strongly attracted to one another. Longer contact time enhanced the attraction between chitosan beads and RO16 dye which allowed the RO16 dye to engage with chitosan more thoroughly and efficiently. As time goes on, the trend slowed down as there are more and more attachment of RO16 on chitosan beads which then resulted in saturation of the active sites. To be more precise, there were not enough binding sites for the adsorption to be occurred towards the end of the process. Increasing the contact time in this stage would not significantly affect adsorption when the saturation of the active sites had been reached. The active sites of chitosan beads now became the limiting factor.

For the three concentrations of dye, a similar trend of increasing amount of dye uptake over time was shown. When the initial concentration of RO16 dyes was increased from 25 mg/L to 100 mg/L, an increased in the amount of dye uptake was observed. The increasing dye concentration resulted in more dye molecules in the system, which provides a stronger driving force to overcome the mass transfer resistance of RO16 towards the chitosan beads. A higher dye concentration also improved the interaction between the chitosan beads and RO16, which would then facilitated the adsorption, leading to an elevated adsorption capacity of RO16 onto the chitosan beads. Similar trend was observed by Chiou and Li (2003) who studied on the elimination of reactive red 189 dye by utilizing cross-linked chitosan beads.

#### **4.2.2 Effect of adsorbent dosage**

The uptake removal of RO16 by various dosage of chitosan beads was shown in Figure 4.2.2. Analyzing the impact of adsorbent dosage helps to determine an adsorbent's efficacy as well as a dye's capacity to be adsorbed at a low dose. In order to investigate how adsorbent dose affects the adsorption process, the dosage of chitosan beads utilized was adjusted from 0.025 g to 0.10 g. It was cleared from the bar chart that the uptake removal increased as the dosage of chitosan beads increased. When the amount of chitosan beads was increased from 0.025 g to 0.10 g, it can be observed that the uptake removal of RO16 increased from 41.0 % to 75.4 %. A decrease in the uptake of dye when a lower dosage of chitosan beads was used can be attributed by the lower amount of binding sites for RO16. In contrast, increasing the amount of chitosan beads in

the system undoubtedly indicated that the number of free available adsorption sites for binding of RO16 dye also became greater. When there are more binding sites available, this situation resulted in more amount of active site and the overall surface area accessible for adsorption, which increases the likelihood of RO16 interact with the sites of chitosan beads (Salleh et al., 2011). Hence, this resulted in higher adsorption rate and consequently, in the uptake removal of RO16 by chitosan beads. Similar trend was noticed in the research done by Khosla, Kaur and Dave (2013).

#### **4.2.3 Effect of agitation rate**

The impact of three agitation rates (100 rpm, 150 rpm and 200 rpm) at various contact time for the removal of RO16 was analyzed. Figure 4.2.3 shows the variation of RO16 dye uptake with agitation rate. The uptake removal of RO16 at the first 5 minutes for 100 rpm, 150 rpm and 200 rpm were only 1.19%, 1.78% and 2.17%, respectively. With increasing time and agitation rates from 100 rpm to 200 rpm, chitosan beads were able to achieve the uptake removal of 58.1% and 63.2%, respectively. Figure 4.2.3 clearly showed that the adsorption was dependent on the agitation rate, whereby an increase in uptake removal of RO16 was observed as the speed of agitation increased from 100 rpm to 200 rpm. The reason for this situation could be related to the RO16 dye molecules diffusing more quickly from the bulk liquid phase into the boundary film layer around the chitosan beads. In other words, this phenomenon can be explained in which an increase in agitation rate decreased the boundary layer's thickness around the particles, enhancing the external mass transfer coefficient and turbulence in the

system. Increasing agitation rate not only minimized the boundary layer resistance, also increased the system's mobility which allowed a better interaction between the RO16 and chitosan beads in the system. Consequently, this resulted in a faster adsorption of dye molecules and improved the efficiency of the adsorption performance to achieve a better uptake. Nandi et al. (2008) utilized kaolin for the removal of crystal violet dye and reported similar trends under the effect of agitation rate.

#### **4.2.4 Effect of pH**

The influence of pH values varying from 3 to 10 towards the ability of chitosan beads to adsorb RO16 was studied in this work and presented in Figure 4.2.4. The adsorption process was strongly influenced by the solution's pH as pH can affect the surface characteristics of adsorbent, dissociation of different functional groups on the vacant site and degree of ionization, making it a crucial factor in the adsorption process. Dye sorption is relied on the protonation and deprotonation of certain functional group since every dye has their preferred specific pH value.

Based on Figure 4.2.4, the system was able to achieve the highest dye uptake at pH 3. Under extremely basic conditions like pH 11 and 12, RO16 dye solution experienced a colour change and became a dark reddish-brown colour solution. This indicated that RO16 dye solution were not suitable to be examined under these pH values. Tay (2011) also reported the similar observation and stated that the irreversible change in colour of RO16 indicated a structural alteration in the

RO16 molecules which is not suitable to be studied. At pH 3, the percentage removal of RO16 was successfully achieved up to 92.5%. A decreasing trend was observed when the pH increased from pH 3 to 10. Sangavi et al. (2020) and Tay (2011) who studied on the adsorption of reactive dyes also reported the similar downtrend. The uptake removal of RO16 decreased to only 3.7% at pH 10, a highly alkaline solution. The surface characteristics and physical strength of chitosan beads have been found to be significantly impacted by the addition of acid. The action of pH towards adsorption performance is closely correlated to the point of zero charge,  $pH_{pzc}$  of chitosan beads. The  $pH_{pzc}$  of chitosan was determined to be at pH 6.57. This value matched closely to the previously reported studies carried out by Kausar et al. (2019) and Chung and Ong (2021) which reported the  $pH_{pzc}$  of 7.00 and 6.90, respectively. The surface of the adsorbent is negatively charged when the pH values examined were more than  $pH_{pzc}$  and may interact with positive dye species; conversely, when the pH values appeared to be lower than  $pH_{pzc}$ , the chitosan is positively charged and may attracted to the negatively charged species. Chitosan consists of amine functional group which can participate actively in the protonation and deprotonation process under different pH values.

From the results, the best uptake occurred at the lowest pH. At low pH condition, protonation of chitosan's amine functional group can take place and there will be as a strong electrostatic interaction occurred between the negatively charged RO16 and positively charged chitosan surface. Conversely, the percentage removal began to decrease as the pH increase. This was linked to the presence of negatively charge chitosan beads at higher pH which leads to the electrostatic

repulsion between the negatively charged chitosan and RO16 dye molecule. Subsequently, the adsorption was hindered and resulted in a declining trend of uptake removal of RO16. RO16 dye adsorption is not promoted by an alkaline pH condition. A significant reduction was observed at pH 8 and this may be due to the surface charge of chitosan being much more negative and caused a strong electrostatic repulsion.

### **4.3 Adsorption isotherm**

Studies on adsorption isotherms are important to explain the mechanism involved between the adsorbate and adsorbent. Understanding of the adsorption isotherm is vital to explain how solutes interact with the adsorbents and to maximize adsorbent utilization. With the aid of adsorption isotherm models, the maximum adsorption capacity can be ascertained, which is useful for assessing how well the adsorbents work. Many isotherm models are typically employed to correlate isotherm data and the adsorption behavior is evaluated using the model that fits the data the best.

Several adsorption isotherms models were employed in this work to describe the equilibrium data, including the Langmuir, Freundlich, and Brunauer-Emmett-Teller (BET) isotherms.

### 4.3.1 Langmuir isotherm

Langmuir isotherm fundamentally offers a key foundation for characterizing the degree and potency of adsorption on the chitosan surface in this investigation. By applying the kinetic theory of gases, Irving Langmuir, a chemist from United States, derived Langmuir adsorption isotherm under the following postulations which included, adsorption is solely composed of a monolayer at the surface; one adsorbed molecule can only reside at a single adsorption site, and there is no intermolecular contact between molecules on different sites; the heat of adsorption is also constant regardless of the number of sites in a monolayer (Langmuir, 1918).

Langmuir adsorption isotherm model is defined and represented by:

$$q_e = \frac{q_m K_L C_e}{1 + K_L C_e} \quad [4.1]$$

Equation 4.1 could be linearized and the equation in linear form is as followed:

$$\frac{C_e}{q_e} = \frac{1}{q_m K_L} + \frac{C_e}{q_m} \quad [4.2]$$

where  $C_e$  = Concentration of RO16 dye at equilibrium (mg/L),  $q_e$  = Amount of RO16 dye adsorbed at equilibrium (mg/g),  $q_m$  = maximum adsorption capacity of chitosan beads (mg/g),  $K_L$  = Langmuir isotherm constant related to energy of chitosan beads (L/mg)

Based on the equation 4.2, a plot of  $\frac{C_e}{q_e}$  versus  $C_e$  representing Langmuir plot was constructed. Figure 4.3.1 depicts the Langmuir isotherm plot for the removal of RO16 using chitosan beads. According to the equation, the gradient of the graph is useful in determining the value of  $q_m$  whereas y-intercept from the graph is

important in calculating the value of  $K_L$ . The Langmuir plot was able to give a coefficient of determination,  $R^2$  value of 0.9940 which considered a good fit in which monolayer adsorption took place on a homogeneous surface. Based on the Figure 4.3.1, the gradient was found to be 0.0262 and y-intercept has the value of 0.4976. Thus, the Langmuir isotherm constant,  $K_L$  and maximum adsorption capacity of chitosan beads were computed and calculated to be 0.05265 L/mg and 38.17 mg/g, respectively.

The following equation defines the separation factor ( $R_L$ ), sometimes referred to as equilibrium parameter, which is a dimensionless constant, is a useful tool for representing the key features of Langmuir isotherm. The following formula can be used to find the dimensionless adsorption constant value:

$$R_L = \frac{1}{1 + K_L C_o} \quad [4.3]$$

where  $R_L$  = equilibrium parameter,  $K_L$  = Langmuir isotherm constant linked to energy of chitosan beads (L/mg),  $C_o$  = Initial concentration of RO16 dye (mg/L)

The effect of shape of isotherm on whether adsorption is favourable or unfavourable was investigated.

#### **4.3.2 Freundlich isotherm**

As opposed to the Langmuir isotherm, the Freundlich isotherm model is applied to multilayer adsorption on heterogeneous sites. It makes the assumption that there are non-uniform affinities and heat distribution during adsorption.



Freundlich isotherm is typically employed for nonideal adsorption on heterogeneous surfaces and assumes that there are numerous and diverse types of accessible sites, each operating simultaneously with different free energies of adsorption (Freundlich, 1906).

The Freundlich isotherm model is depicted as follows:

$$q_e = K_F C_e^{\frac{1}{n}} \quad [4.4]$$

When the Freundlich isotherm equation is linearized by taking logarithm on both sides, it is presented in the following equation:

$$\log q_e = \frac{\log C_e}{n} + \log K_F \quad [4.5]$$

where  $q_e$  = amount of RO16 dye adsorbed at equilibrium (mg/g),  $C_e$  = concentration of RO16 at equilibrium (mg/L),  $n$  = Freundlich constant for intensity,  $K_F$  = Freundlich isotherm constant for adsorption capacity

Based on the equation 4.5, a plot of  $\log q_e$  against  $\log C_e$  can be constructed. Figure 4.3.2 shows the Freundlich isotherm plot on the removal of RO16 by chitosan beads. A coefficient of determination,  $R^2$  value of 0.9790 was obtained. The y-intercept and gradient are useful in determining the  $n$  and  $K_F$  values, respectively. The adsorption process is deemed favourable if the  $n$  value falls between 1 and 10. Based on the calculation, it was found that the  $n$  and  $K_F$  values were 2.4710 and 5.2493 mg/g, respectively. This again supported the finding that this adsorption process is a promising method for the removal of RO16.

### 4.3.3 Brunauer-Emmett-Teller (BET) isotherm

Brunauer-Emmett-Teller (BET) model is a modified version for Langmuir isotherm that takes into account multilayers of coverage, which are not permitted in the Langmuir model. The assumption behind this model is physisorption leads to the formation of multilayer adsorption. Additionally, the theory suggested that adsorption at one site is independent of adsorption at other site and that the solid surface contains homogeneous adsorption sites. Following the formation of the monolayer, the adsorption process can proceed to form the second, third, and so on layers of a multilayer. Besides, the adsorption energy at each surface site is the same for the adsorbate (Brunauer, Emmett and Teller, 1938).

The Brunauer-Emmett-Teller (BET) isotherm model is expressed as the following equation:

$$q_e = \frac{K_B q_m C_e}{(C_s - C_e) \left[ 1 + (K_B - 1) \left( \frac{C_e}{C_s} \right) \right]} \quad [4.6]$$

The equation of BET model in linear form is represented as:

$$\frac{C_e}{(C_s - C_e) q_e} = \left( \frac{K_B - 1}{K_B q_m} \right) \left( \frac{C_e}{C_s} \right) + \frac{1}{K_B q_m} \quad [4.7]$$

where  $q_e$  = amount of RO16 dye adsorbed at equilibrium (mg/g),  $K_B$  = BET constant which describes the energy involved in the adsorbate-adsorbent interaction,  $q_m$  = amount of RO16 dye in formation of complete monolayer (mg/g),  $C_e$  = concentration of RO16 dye at equilibrium (mg/L),  $C_s$  = RO16 concentration at saturation (mg/L)

By comparing the  $R^2$  value for all isotherm models, it can be seen that both Langmuir and BET isotherm model demonstrated higher correlation of determination in the adsorption by chitosan beads compared to Freundlich isotherm model. The results obtained indicated that monolayer adsorption occurred on a uniform adsorbent surface with a limited number of adsorption sites. Nevertheless, conformity to BET isotherm model also implied that the adsorption of RO16 was extended beyond monolayer coverage.

#### **4.4 Adsorption kinetics studies**

Adsorption kinetics defines the rate at which a solute is retained or released at specific dosage of adsorbent, pH, flow rate and temperature from an aqueous environment to the solid-phase interface (William Kajjumba et al., 2019). Important insights into probable adsorption mechanism and their potential rate-limiting step are able to gain from adsorption kinetics. To determine the adsorption kinetics model, the experimental results from the adsorption of chitosan beads were analyzed using pseudo-first and pseudo-second order kinetic models. The model that best represents the adsorption process is determined by comparing the linear regression coefficient of determination, or  $R^2$  value that evaluates the accuracy of a statistical model's prediction of a result.

##### **4.4.1 Pseudo-first order kinetics model**

The Lagergren pseudo-first order model, commonly utilized during the initial phase of adsorption processes, operates on the premise that the difference

between saturation concentration and the quantity of solid adsorbed is directly proportional to the rate at which solute is absorbed over time (Sahoo and Prelot, 2020). This model accurately describes kinetics in scenarios where adsorption occurs via diffusion through the interface. In general, physisorption limited the rate at which particles adsorb onto the adsorbent in pseudo-first order model (Lagergren, 1898).

The pseudo-first order kinetic model is written as:

$$\frac{dq}{dt} = k_1(q_e - q_t) \quad [4.8]$$

By applying boundary conditions and integration, the pseudo-first order model equation in linearized form is as follows:

$$\log(q_e - q_t) = \log q_e - \frac{k_1}{2.303}t \quad [4.9]$$

where  $q_e$  = amount of RO16 adsorbed at equilibrium (mg/g),  $q_t$  = amount of RO16 adsorbed at time  $t$  (mg/g),  $k_1$  = pseudo-first order kinetics rate constant ( $\text{min}^{-1}$ ),  $t$  = time (minutes)

Based on the equation 4.9, a graph of  $\log (q_e - q_t)$  versus  $t$  for different concentrations of dye (25 mg/L and 100 mg/L) was constructed. Figure 4.4.1 shows the pseudo-first order plot for the removal of RO16 by chitosan beads. According to the equation, the y-intercept and gradient from graph provided the information to obtain the value of  $q_e$  and  $k_1$ , respectively. For each concentration of dye, the value of  $R^2$ ,  $q_e$  and  $k_1$  were calculated and obtained. The value of experimental  $q_e$ , calculated  $q_e$ ,  $k_1$  and  $R^2$  were tabulated in Table 4.4. The

calculated equilibrium adsorption capacity exhibited a deviation from the experimentally values. By referring to Table 4.4, the  $R^2$  values for RO16 concentrations under study were considered low as both were below 0.96. Besides, the experimental data did not match this model very well too. It was therefore determined that this model was unsuitable to represent the adsorption of RO16 utilizing the chitosan beads.

#### 4.4.2 Pseudo-second order kinetics model

Ho's pseudo-second order kinetic model was employed to conduct further analysis on the kinetic data. The adsorption is assumed to follow second order chemisorption in this model. In this case, the adsorption capacity governs the adsorption rate rather than the adsorbate concentration. The related equation can be represented as:

$$\frac{dq_t}{dt} = k_2(q_e - q_t)^2 \quad [4.10]$$

After integrating and taking into consideration the boundary conditions, the final equation is:

$$\frac{t}{q_t} = \frac{1}{h} + \frac{t}{q_e} \quad [4.11]$$

$$\text{with } h = k_2 q_e^2 \quad [4.12]$$

where  $q_t$  = amount of RO16 adsorbed at time  $t$  (mg/g),  $k_2$  = pseudo-second order kinetics rate constant (g/mg min),  $q_e$  = amount of RO16 adsorbed at equilibrium (mg/g),  $h$  = initial adsorption rate (mg/g min)

According to the equation 4.11, a plot of  $\frac{t}{q_t}$  against  $t$  at 25 mg/L and 100 mg/L of RO16 dye was constructed. Figure 4.4.2 presents the pseudo-second order plot for the adsorption of RO16 onto chitosan beads. For each concentration of dye, the value of  $k_2$ ,  $q_e$ ,  $h$  and  $R^2$  were calculated and tabulated in Table 4.4. The calculated equilibrium adsorption capacity also exhibited a deviation from those obtained experimentally. However, it was clearly observed that the  $R^2$  value for pseudo-second order model was higher than the pseudo-first order kinetic model. This indicated that the experimental data fitted and matched with this model better compared to pseudo-first order kinetic model. When fitting the data to a pseudo second-order model, it suggests that the rate of occupied active sites is proportional with the square of the number of unadsorbed sites (Abia and Onwu, 2010). It is therefore proposed that the rate-determining step may be chemisorption or chemical adsorption where the adsorbent and adsorbate share or exchange electrons to create valency forces (Ho and McKay, 1999).

Besides, the value of pseudo-second order rate constant was found to decrease from  $5.5707 \times 10^{-4}$  to  $8.0773 \times 10^{-5}$  as the concentration of RO16 dye increased. This demonstrated that the adsorption rate was slower at higher initial RO16 concentration. This behaviour could be justified by the fact that at lower concentrations, the adsorption surface site has lesser competition. In contrast, increased in concentrations caused more competition for the surface active sites, which will then slow down the rate of adsorption (Chen and Zhao, 2009).

In many studies, the pseudo-second order kinetic model frequently exhibited great correlations with the adsorption system of dyes, such as in the studies from Haya Alyasi, Mackey and McKay (2023) who utilized chitosan in adsorption of methyl orange; adsorption of malachite green by maize cob (Sonawane and Shrivastava, 2009); Ghanizadeh and Asgari (2010) on the adsorption study of methylene blue using bone charcoal and Foroughi-Dahr et al. (2014) who utilized tea waste for the removal of Congo red.

The values of  $q_e$ ,  $k_2$  and  $h$  obtained from pseudo-second order kinetic model is useful in the theoretical model for RO16 dye. The provided equation offers a versatile framework for constructing predictive models for RO16 adsorption, accommodating various contact times and initial concentrations within the specified range.

The theoretical adsorption capacity for RO16 adsorption was calculated and obtained from the equation. Figure 4.4.3 displayed the comparison between theoretical model developed for RO16 using chitosan beads with actual experimental results. Based on the figure, at low concentration which is 25 mg/L, the theoretical data was still considered agreed well with the experimental data as it does not undergo large deviation where the theoretical and experimental adsorption capacity in 360 minutes were determined to be 6.7522 mg/g and 8.6265 mg/g, respectively. However, the deviation was enlarged when the concentration increased to 100 mg/L. Such discrepancy might be resulted from the multilayer formation on chitosan beads when the concentration of RO16 increases. The uptake of RO16 by rice hulls treated with ethylenediamine exhibited similar phenomenon (Ong, Lee and Zainal, 2007).



## CHAPTER 5

### CONCLUSION

#### 5.1 Conclusion

In the current work, chitosan beads clearly demonstrated that it could be a potentially useful and low-cost adsorbent in the removal of RO16. The significant functional group involved in the adsorption of RO16 was studied using ATR-FTIR. Some of the peaks shifted after the adsorption process and this indicated that these functional groups were responsible for the interaction between RO16 and chitosan beads. AFM and SEM analysis demonstrated notable changes in the surface topography and morphology of the chitosan beads, further confirming the efficacy of the adsorption process. The uptake removal of RO16 increased with increased contact time, agitation rate, amount of chitosan beads and decreased with pH and initial concentration of RO16. Besides, the equilibrium adsorption data was determined to be well-suited to both Langmuir and BET isotherm models compared to Freundlich isotherm model. The maximum adsorption capacity of 38.17 mg/g with  $R^2$  value of 0.9940 were obtained. The kinetic study results obeyed to the pseudo-second order kinetic model. Plackett-Burman design identified pH and contact time as the significant factors in the adsorption of RO16. By using RSM, the optimum conditions where the maximum RO16 removal was obtained at 360 minutes, pH 3, 0.05 g of chitosan beads, 100 mg/L of RO16 concentration and at 150 rpm of agitation rate. Under these optimum conditions, the uptake removal of 94.55% was

attainable, which further proven the capabilities of chitosan beads in removing dyes in wastewater.

## **5.2 Future Prospects**

Chitosan bead has proven to be having a great potential as an efficient adsorbent in removing dye from aqueous solution. Further studies can be performed involving the removal of other contaminants such as heavy metal ions, antibiotics, or even other type of dyes to evaluate its adsorption performance. Besides, chemical modification such as modifying the surface functional group of chitosan or copolymerized it with other polymer could be done to enhance its adsorption capacity and affinity. Desorption process can also be studied in order to evaluate the feasibility of using chitosan beads for multiple adsorption cycles. Column studies can be conducted as well to obtain design that would be applicable to commercial system.

## REFERENCES

Abdeen, Z. and G. Mohammad, S., 2014, Study of the adsorption efficiency of an eco-friendly carbohydrate polymer for contaminated aqueous Solution by organophosphorus pesticide. *Open Journal of Organic Polymer Materials*, 04(01), pp.16–28. doi:<https://doi.org/10.4236/ojopm.2014.41004>.

Abdulhameed, A.S., Mohammad, A.T. and Jawad, A.H., 2019, Application of response surface methodology for enhanced synthesis of chitosan tripolyphosphate/TiO<sub>2</sub> nanocomposite and adsorption of reactive orange 16 dye. *Journal of Cleaner Production*, 232, pp.43–56. doi:<https://doi.org/10.1016/j.jclepro.2019.05.291>.

Abel, A., 2012, The history of dyes and pigments. *Colour Design*, 557–587. doi:[10.1016/b978-0-08-101270-3.00024-2](https://doi.org/10.1016/b978-0-08-101270-3.00024-2)

Abia, A.A. and Onwu, F.K., 2010, Sorption kinetics of Ni<sup>2+</sup>, Cd<sup>2+</sup> and Pb<sup>2+</sup> by African white star apple (*chrysophyllum albidum*) shell. *Journal of Research in Physical Sciences*. 6(2), pp.64-70.

Agarwal, A.K., Kadu, M.S., Pandhurnekar, C.P., Muthreja, I.L., 2014, Langmuir, Freundlich and BET adsorption isotherm studies for zinc ions onto coal fly ash. *International Journal of Application or Innovation in Engineering & Management*, 3(1), pp.64-71.

Ali, Karthikeyan, K., Sentamil Selvan M, Kumar Mithilesh, Madhangi Priyadharshini, N. Maheswari, Janani Sree G, Padmanaban, V.C. and Ram Sharan Singh., 2018, Removal of Reactive Orange 16 by adsorption onto

activated carbon prepared from rice husk ash: statistical modelling and adsorption kinetics. 55(1), pp.26–34. doi:<https://doi.org/10.1080/01496395.2018.1559856>.

Arami, M., Limaee, N.Y., Mahmoodi, N.M. and Tabrizi, N.S., 2005, Removal of dyes from colored textile wastewater by orange peel adsorbent: equilibrium and kinetic studies. *Journal of Colloid and Interface Science*, [online] 288(2), pp.371–376. doi:<https://doi.org/10.1016/j.jcis.2005.03.020>.

Bassi, R., Prasher, S.O. and Simpson, B.K., 2000, Removal of selected metal ions from aqueous solutions Using chitosan flakes. *Separation Science and Technology*, 35(4), pp.547–560. doi:<https://doi.org/10.1081/ss-100100175>.

Bernard, J.P., 2018, A Brief History of Synthetic Dyes - First Source Worldwide, LLC. [online] First Source Worldwide. Available at: <https://www.fsw.cc/synthetic-dyes-history/>.

Bhatt, R., Sreedhar, B. and Padmaja, P., 2015, Adsorption of chromium from aqueous solutions using crosslinked chitosan–diethylenetriaminepentaacetic acid. *International Journal of Biological Macromolecules*, 74, pp.458–466. doi:<https://doi.org/10.1016/j.ijbiomac.2014.12.041>.

Box, G. E. P. and Wilson, K. B., 1951, On the Experimental Attainment of Optimum Conditions. *Journal of the Royal Statistical Society. Series B (Methodological)*, 13(1), 1-45.

Brunauer, S., Emmett, P. H. and Teller, E., 1938. Adsorption of Gases in Multimolecular Layers. *Journal of the American Chemical Society*, 60, pp. 309 – 319.

Chan, K.T., Ong, S.T. and Ha, S.T., 2024, Adsorptive removal of Congo Red dye from its aqueous solutions by tetraethylenepentamine modified peanut husks composite beads. *Desalination and water treatment*, 317, pp.100060–100060. doi:<https://doi.org/10.1016/j.dwt.2024.100060>.

Chatterjee, S., Chatterjee, S., Chatterjee, B.P. and Guha, A.K., 2007, Adsorptive removal of congo red, a carcinogenic textile dye by chitosan hydrobeads: Binding mechanism, equilibrium and kinetics. *Colloids and Surfaces A: Physicochemical and Engineering Aspects*, 299(1-3), pp.146–152. doi:<https://doi.org/10.1016/j.colsurfa.2006.11.036>.

Chauhan, K., Trivedi, U., and Patel, K.C., 2006, Application of response surface methodology for optimization of lactic acid production using date juice. *J. Microb. Biotechnol.*, 16, pp. 1410–1415

Chen, H. and Zhao, J., 2009, Adsorption study for removal of Congo red anionic dye using organo-attapulgitite. *Adsorption*, 15(4), pp.381–389. doi:<https://doi.org/10.1007/s10450-009-9155-z>.

Cheung, W.H., Szeto, Y.S. and McKay, G., 2009, Enhancing the adsorption capacities of acid dyes by chitosan nano particles. *Bioresource Technology*, 100(3), pp.1143–1148. doi:<https://doi.org/10.1016/j.biortech.2008.07.071>.

Chiou, M.S. and Chuang, G.S., 2006, Competitive adsorption of dye metanil yellow and RB15 in acid solutions on chemically cross-linked chitosan beads. *Chemosphere*, 62(5), pp.731–740. doi:<https://doi.org/10.1016/j.chemosphere.2005.04.068>.

Chiou, M.S. and Li, H.Y., 2003, Adsorption behavior of reactive dye in aqueous solution on chemical cross-linked chitosan beads. *Chemosphere*, 50(8), pp.1095–1105. doi:[https://doi.org/10.1016/s0045-6535\(02\)00636-7](https://doi.org/10.1016/s0045-6535(02)00636-7).

Chiou, M.S., Kuo, W.S. and Li, H.Y., 2003, Removal of reactive dye from wastewater by adsorption using ECH cross-linked chitosan beads as medium. *Journal of Environmental Science and Health, Part A*, 38(11), pp.2621–2631. doi:<https://doi.org/10.1081/ese-120024451>.

Chung, W.Y. and Ong, S.T., 2021. Effective removal of Reactive Brown 10 from aqueous solution by using chitosan beads: Batch and experimental design studies. *Journal of Physical Science*, 32(1), pp.91–108. doi:<https://doi.org/10.21315/jps2021.32.1.7>.

Dotto, G.L. and Pinto, L.A.A., 2011, Adsorption of food dyes onto chitosan: Optimization process and kinetic. *Carbohydrate Polymers*, 84(1), pp.231–238. doi:<https://doi.org/10.1016/j.carbpol.2010.11.028>.

Doulati Ardejani, F., Badii, Kh., Yousefi Limaee, N., Mahmoodi, N.M., Arami, M., Shafaei, S.Z. and Mirhabibi, A.R., 2007, Numerical modelling and laboratory studies on the removal of Direct Red 23 and Direct Red 80 dyes from textile effluents using orange peel, a low-cost adsorbent. *Dyes and Pigments*, 73(2), pp.178–185. doi:<https://doi.org/10.1016/j.dyepig.2005.11.011>.

FAO., 2022, *The State of World Fisheries and Aquaculture 2022*. FAO. doi:<https://doi.org/10.4060/cc0461en>.

Fernandes Queiroz, M., Melo, K., Sabry, D., Sasaki, G. and Rocha, H., 2014, Does the use of chitosan contribute to oxalate kidney stone formation? *Marine Drugs*, 13(1), pp.141–158. doi:<https://doi.org/10.3390/md13010141>.

Foroughi-Dahr, M., Abolghasemi, H., Esmaili, M., Shojamoradi, A. and Fatoorehchi, H., 2014, Adsorption characteristics of Congo Red from aqueous solution onto tea waste. *Chemical Engineering Communications*, 202(2), pp.181–193. doi:<https://doi.org/10.1080/00986445.2013.836633>.

Freundlich, H. M. F., 1906. Over the Adsorption in Solution. *The Journal of Physical Chemistry*, 57, pp. 385 – 471.

Ghanizadeh, Gh. and Asgari, G., 2010, Adsorption kinetics and isotherm of methylene blue and its removal from aqueous solution using bone charcoal. *Reaction Kinetics, Mechanisms and Catalysis*, 102(1), pp.127–142. doi:<https://doi.org/10.1007/s11144-010-0247-2>.

Golfer Muedas-Taipe, Maza, M., Santillan, F.A., Velásquez, C.J. and Yvan J.O. Asencios., 2020, Removal of azo dyes in aqueous solutions using magnetized and chemically modified chitosan beads. *Materials Chemistry and Physics*, 256, pp.123595–123595. doi:<https://doi.org/10.1016/j.matchemphys.2020.123595>.

Gregory, A.R., Elliot, S. and Kludge, P., 1991. Ames testing of direct black 3B parallel carcinogenic. *Journal Applied Toxicology*, 1, pp. 308-313.

Gunasegaran, M., Ravi, S. and Shoparwe, N.F., 2020, Kinetic studies of Reactive Orange 16 (RO16) dye removal from aqueous solution using PIMs. *Journal of Physics: Conference Series*, 1529, p.052003. doi:<https://doi.org/10.1088/1742-6596/1529/5/052003>.

Gupta, S., Kumar, D. and Gaur, J.P., 2009, Kinetic and isotherm modeling of lead(II) sorption onto some waste plant materials. *Chemical Engineering Journal*, 148(2-3), pp.226–233. doi:<https://doi.org/10.1016/j.cej.2008.08.019>.

Hameed, B.H., Krishni, R.R. and Sata, S.A., 2009, A novel agricultural waste adsorbent for the removal of cationic dye from aqueous solutions. *Journal of Hazardous Materials*, 162(1), pp.305–311. doi:<https://doi.org/10.1016/j.jhazmat.2008.05.036>.

Haya Alyasi, Mackey, H.R. and McKay, G., 2023, Adsorption of Methyl Orange from water using chitosan bead-like materials. *Molecules*, 28(18), pp.6561–6561. doi:<https://doi.org/10.3390/molecules28186561>.

Ho, Y., 2000, The kinetics of sorption of divalent metal ions onto sphagnum moss peat. *Water Research*, 34(3), pp.735–742. doi:[https://doi.org/10.1016/s0043-1354\(99\)00232-8](https://doi.org/10.1016/s0043-1354(99)00232-8).

Jain, R., Sharma, P., Sikarwar, S., Mittal, J. and Pathak, D., 2013, Adsorption kinetics and thermodynamics of hazardous dye Tropaeoline 000 onto Aeroxide Alu C (Nano alumina): a non-carbon adsorbent. *Desalination and Water Treatment*, 52(40-42), pp.7776–7783. doi:<https://doi.org/10.1080/19443994.2013.837009>.

Jamee, R. and Siddique, R., 2019, Biodegradation of synthetic dyes of textile effluent by microorganisms: An environmentally and economically sustainable approach. *European Journal of Microbiology and Immunology*, 9(4), pp. 114–118. doi:[10.1556/1886.2019.00018](https://doi.org/10.1556/1886.2019.00018).



Karnitz, O., Gurgel, L.V.A., de Melo, J.C.P., Botaro, V.R., Melo, T.M.S., de Freitas Gil, R.P. and Gil, L.F., 2007, Adsorption of heavy metal ion from aqueous single metal solution by chemically modified sugarcane bagasse. *Bioresource Technology*, 98(6), pp.1291–1297. doi:<https://doi.org/10.1016/j.biortech.2006.05.013>.

Kausar, A., Naeem, K., Hussain, T., Nazli, Z.-H., Bhatti, H.N., Jubeen, F., Nazir, A. and Iqbal, M., 2019, Preparation and characterization of chitosan/clay composite for direct Rose FRN dye removal from aqueous media: comparison of linear and non-linear regression methods. *Journal of Materials Research and Technology*, 8(1), pp.1161–1174. doi:<https://doi.org/10.1016/j.jmrt.2018.07.020>.

Khosla, E., Kaur, S. and Dave, P.N., 2013, Tea waste as adsorbent for ionic dyes. *Desalination and Water Treatment*. 51(34-36), pp.6552–6561. doi:<https://doi.org/10.1080/19443994.2013.791776>.

Lagergren, S.K., 1898, About the Theory of So-Called Adsorption of Soluble Substances. 24(4), pp.1–39.

Langmuir, I., 1918, THE ADSORPTION OF GASES ON PLANE SURFACES OF GLASS, MICA AND PLATINUM. *Journal of the American Chemical Society*, 40(9), pp.1361–1403. doi:<https://doi.org/10.1021/ja02242a004>.

Lee, S.M. and Ong, S.T., 2014, Oxalic Acid Modified Rice Hull as a sorbent for Methylene Blue removal. *APCBEE Procedia*, 9, pp.165–169. doi:<https://doi.org/10.1016/j.apcbee.2014.01.029>.

Li, H., Miao, L., Zhao, G., Jia, W. and Zhu, Z., 2022, Preparation of high-performance chitosan adsorbent by cross-linking for adsorption of Reactive Red

2 (RR2) dye wastewater. *Journal of Environmental Chemical Engineering*, 10(6), pp.108872–108872. doi:<https://doi.org/10.1016/j.jece.2022.108872>.

Liang, S., Guo, X., Feng, N. and Tian, Q., 2009, Application of orange peel xanthate for the adsorption of  $Pb^{2+}$  from aqueous solutions. *Journal of Hazardous Materials*, 170(1), pp.425–429. doi:<https://doi.org/10.1016/j.jhazmat.2009.04.078>.

Malakootian, M. and Heidari, M.R., 2018. Reactive orange 16 dye adsorption from aqueous solutions by psyllium seed powder as a low-cost biosorbent: Kinetic and equilibrium studies, *Applied Water Science*, 8(7). doi:[10.1007/s13201-018-0851-2](https://doi.org/10.1007/s13201-018-0851-2).

Marrakchi, F., Ahmed, M.J., Khanday, W.A., Asif, M. and Hameed, B.H., 2017, Mesoporous carbonaceous material from fish scales as low-cost adsorbent for reactive orange 16 adsorption. *Journal of the Taiwan Institute of Chemical Engineers*, 71, pp.47–54. doi:<https://doi.org/10.1016/j.jtice.2016.12.026>.

Myers, R.H. and Montgomery, D.C., 2002, *Response Surface 1 Methodology – Process and Product Optimization using designed experiments*. 2nd edn. New York: John Wiley & Sons.

Nandi, B.K., Goswami, A., Das, A.K., Mondal, B. and Purkait, M.K., 2008, Kinetic and equilibrium studies on the adsorption of Crystal Violet dye using kaolin as an adsorbent. *Separation Science and Technology*, 43(6), pp.1382–1403. doi:<https://doi.org/10.1080/01496390701885331>.

Ngah, W.S.W. and Fatinathan, S., 2010, Adsorption characterization of Pb(II) and Cu(II) ions onto chitosan-tripolyphosphate beads: Kinetic, equilibrium and

thermodynamic studies. *Journal of Environmental Management*, 91(4), pp.958–969. doi:<https://doi.org/10.1016/j.jenvman.2009.12.003>.

Obaid, M.K., Abdullah, L.C. and Idan, I.J., 2016. Removal of reactive Orange 16 dye from aqueous solution by using modified Kenaf Core Fiber, *Journal of Chemistry*, 2016, pp. 1–7. doi:10.1155/2016/4262578.

Ong, P.S., Ong, S.T. and Hung, Y.T., 2013, Utilization of mango leaf as a low-cost adsorbent for the removal of Cu(II) ions from aqueous solution. *Asian Journal of Chemistry*, 25(11), pp.6141–6145. doi:<https://doi.org/10.14233/ajchem.2013.14290>.

Ong, S.T and Seou, C. K., 2013, Removal of reactive black 5 from aqueous solution using chitosan beads: optimization by Plackett–Burman design and response surface analysis. *Desalination and Water Treatment*, 52(40-42), pp.7673–7684. doi:<https://doi.org/10.1080/19443994.2013.830684>.

Ong, S.T. and Lee, W.N., 2015, Evaluation on the efficiency of ethylenediaminetetraacetic acid (EDTA)-modified rice husk as a low-cost sorbent for various dyes removal under continuous flow condition. *Desalination and Water Treatment*, 57(39), pp.18157–18167. doi:<https://doi.org/10.1080/19443994.2015.1088474>.

Ong, S.T., Ha, S.T., Khoo, E.C. and Hii, S.L., 2013, Nitrilotriacetic acid modified sugarcane bagasse in the removal of basic blue 3 from aqueous environment. *International Journal of Environmental Engineering*, 5(3), p.299. doi:<https://doi.org/10.1504/ijee.2013.054704>.

Ong, S.T., Khoo, E.C., Keng, P.S., Hii, S.L., Lee, S.L., Hung, Y.T. and Ha, S.T., 2011, Plackett–Burman design and response surface methodological approach to optimize basic dyes removal using sugarcane bagasse. *Desalination and Water Treatment*, 25(1-3), pp.310–318. doi:<https://doi.org/10.5004/dwt.2011.1974>.

Ong, S.T., Lee, C.K. and Zainal, Z., 2007, Removal of basic and reactive dyes using ethylenediamine modified rice hull. *Bioresource Technology*, 98(15), pp.2792–2799. doi:<https://doi.org/10.1016/j.biortech.2006.05.011>.

Pourrahim, S., Salem, A., Salem, S. & Tavangar, R., 2020, Application of solid waste of ductile cast iron industry for treatment of wastewater contaminated by reactive blue dye via appropriate nano-porous magnesium oxide. *Environmental Pollution*, 256, Article 113454. doi : 10.1016/j.envpol.2019.113454

Qaiser, S., Saleemi, A.R. and Umar, M., 2009, Biosorption of lead from aqueous solution by *Ficus religiosa* leaves: Batch and column study. *Journal of Hazardous Materials*, 166(2-3), pp.998–1005. doi:<https://doi.org/10.1016/j.jhazmat.2008.12.003>.

Razmi F.A., Ngadi N., Rahman R.A., Kamaruddin M.J., 2017. Removal of reactive dye using new modified chitosan pandan sorbent, *Chemical Engineering Transactions*, 56, 121-126 DOI:10.3303/CET1756021

Sahoo, T.R. and Prelot, B., 2020, Adsorption processes for the removal of contaminants from wastewater. *Nanomaterials for the Detection and Removal of Wastewater Pollutants*, pp.161–222. doi:<https://doi.org/10.1016/b978-0-12-818489-9.00007-4>.

Salehi, E., Fereshteh Soroush, Momeni, M., Barati, A. and Khakpour, A., 2017, Chitosan/polyethylene glycol impregnated activated carbons: Synthesis, characterization and adsorption performance. *Frontiers of Chemical Science and Engineering*, 11(4), pp.575–585. doi:<https://doi.org/10.1007/s11705-017-1650-2>.

Salih, S.J., Abdul Kareem, A.S. and Anwer, S.S., 2022, Adsorption of anionic dyes from textile wastewater utilizing raw corncob. *Heliyon*, 8(8), p.e10092. doi:<https://doi.org/10.1016/j.heliyon.2022.e10092>.

Salleh, M.A.M., Mahmoud, D.K., Karim, W.A.W.A. and Idris, A., 2011, Cationic and anionic dye adsorption by agricultural solid wastes: A comprehensive review. *Desalination*, 280(1-3), pp.1–13. doi:<https://doi.org/10.1016/j.desal.2011.07.019>.

Sangavi, G., Bakshi, A., Ganapathy, M. and Ganesan, N.D., 2020. Adsorption of reactive dyes from aqueous solution using activated carbon prepared from plantain leaf sheath waste. *Chemical and Biochemical Engineering Quarterly*, (3). doi:<https://doi.org/10.15255/cabeq.2020.1826>.

Saravanan, A., Kumar, P.S., Vo, D.-V.N., Swetha, S., Ngueagni, P.Tsopbou., Karishma, S., Jeevanantham, S. and Yaashikaa, P.R., 2021, Ultrasonic assisted agro waste biomass for rapid removal of Cd(II) ions from aquatic environment: Mechanism and modelling analysis. *Chemosphere*, 271, p.129484. doi:<https://doi.org/10.1016/j.chemosphere.2020.129484>.

Senthil Kumar, P., Joshiba, G.J., Femina, C.C., Varshini, P., Priyadarshini, S., Arun Karthick, M.S. and Jothirani, R., 2019, A critical review on recent developments in the low-cost adsorption of dyes from wastewater. *Desalination*

and Water Treatment, 172, pp.395–416.  
doi:<https://doi.org/10.5004/dwt.2019.24613>.

Sireesha, C., Durairaj, K., Balasubramanian, B., Sumithra, S., Subha, R., Kamyab, H. and Chelliapan, S., 2023, Process development of guava leaves with alkali in removal of zinc ions from synthetic wastewater. Journal of the Taiwan Institute of Chemical Engineers, [online] p.105283.  
doi:<https://doi.org/10.1016/j.jtice.2023.105283>.

Sonawane, G.H. and Shrivastava, V.S., 2009, Kinetics of decolourization of malachite green from aqueous medium by maize cob (*Zea mays*): An agricultural solid waste. Desalination, 247(1-3), pp.430–441.  
doi:<https://doi.org/10.1016/j.desal.2009.01.006>.

Subramani, S.E. and Thinakaran, N., 2017, Isotherm, kinetic and thermodynamic studies on the adsorption behaviour of textile dyes onto chitosan. Process Safety and Environmental Protection, 106, pp.1–10.  
doi:<https://doi.org/10.1016/j.psep.2016.11.024>.

Suteu, D., Zaharia, C. and Malutan, T., 2011, Removal of orange 16 reactive dye from aqueous solutions by waste sunflower seed shells. Journal of the Serbian Chemical Society, 76(4), pp.607–624.  
doi:<https://doi.org/10.2298/jsc100721051s>.

Tarik Ainane, Khammour, F., Talbi, M. and M'hamed Elkouali., 2014, A novel bio-adsorbent of mint waste for dyes remediation in aqueous environments: study and modeling of isotherms for removal of methylene Blue. 30(3), pp.1183–1189. doi:<https://doi.org/10.13005/ojc/300332>.

Tay, C.I. and Ong, S.T., 2019, Guava leaves as adsorbent for the removal of emerging pollutant: Ciprofloxacin from aqueous solution. *Journal of Physical Science*, 30(2), pp.137–156. doi:<https://doi.org/10.21315/jps2019.30.2.8>.

Tay, K.M., 2011. Removal of Reactive orange 16 (RO16) using chemically modified pineapple peels. Degree. Univerisiti Tunku Abdul Rahman. Available at: <http://eprints.utar.edu.my/78/1/CL-2011-0704921-1.pdf>

Vakili, M., Deng, S., Li, T., Wang, W., Wang, W. and Yu, G., 2018, Novel crosslinked chitosan for enhanced adsorption of hexavalent chromium in acidic solution. *Chemical Engineering Journal*, 347, pp.782–790. doi:<https://doi.org/10.1016/j.cej.2018.04.181>.

Vijayalakshmi, K., Devi, B.M., Sudha, P.N., Venkatesan, J., Anil, S., 2016, Synthesis, characterization and applications of nanochitosan/sodium alginate/microcrystalline cellulose film. *Journal of Nanomedicine & Nanotechnology*, 07(06). doi:<https://doi.org/10.4172/2157-7439.1000419>.

William Kajjumba, G., Emik, S., Öngen, A., Kurtulus Özcan, H. and Aydın, S., 2019, Modelling of adsorption kinetic processes—Errors, theory and application. *Advanced Sorption Process Applications*. [online] doi:<https://doi.org/10.5772/intechopen.80495>.

Yildirim, A., 2021. Removal of the anionic dye reactive orange 16 by chitosan/tripolyphosphate/mushroom, *Chemical Engineering & Technology*, 44(8), pp. 1371–1381. doi:10.1002/ceat.202100077.